

# **ISOSPIN DEPENDENCE OF BALANCE ENERGY IN HEAVY ION REACTIONS**

*Thesis submitted in partial fulfillment of the requirement for*

*The award of the degree of*

*Masters of Science*

*In*

**PHYSICS**

Submitted by

**DOLLY SOOD**

**Roll no. - 300804005**

**Under**

**the guidance of**

**Dr. Suneel Kumar**



**School of physics and Material Science**

**Thapar University**

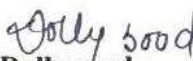
**Patiala – 147004 (PUNJAB)**

**INDIA**

## CERTIFICATE

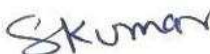
I hereby declare that the report entitled “**Isospin dependence of balance energy using IQMD model**” is an authentic record of my own work carried out as requirements for the award of degree of M. Sc. (Masters of Science) at Thapar University Patiala (Punjab), under the guidance of Dr. Suneel Kumar (SPMS) during January to July 2010. The matter presented in the thesis has not been submitted in part or full for award of any other degree.

**Date: 15/07/2010**

  
**Dolly sood**

Roll No. =300804005

It is certified that the above statement made by the candidate is correct to best of my knowledge and belief.



**(Dr. Suneel Kumar)**

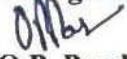
**Assistant professor**

**School of Physics and Material Science,**

**Thapar University**

**Patiala.**

**Countersigned by:**

  
**Dr. O.P. Pandey**

**(Prof. & Head)**

**School of Physics and Materials Science,**

**Thapar University,**

**Patiala.**

  
**Dr. R.K. Sharma**

**Dean of academic Affairs,**

**Thapar University,**

**Patiala**

## *ACKNOWLEDGEMENT*

I owe my deepest gratitude to **Dr. Suneel Kumar**, my worthy supervisor, who has been an inspiration during my research work. Without him, this thesis would not have been possible. I thank him for his patience and encouragement that carried me on through difficult times, and for his insights and suggestions that helped to shape my research skills. I express my sincere thanks to him for his valuable guidance in carrying out work under his effective supervision, encouragement and cooperation. His visionary thoughts have influenced me greatly. His dynamical attitude has empowered me with zeal of energy to conquer the minor details of my research work.

I also thank **Dr. O. P. Pandey**, Professor and Head, School of Physics and Material Science for his support and providing facilities.

A special word of thanks to **Mr. Sanjeev Kumar** and **Mrs. Varinderjit Kaur**, Research Scholars for the help and valuable suggestions whenever I needed out of their busy schedule.

Special thanks are due to all my friends and the staffs at the School of Physics and Material Sciences for providing me a friendly atmosphere and encouraging me throughout this work.

I am deeply thankful to my Family, their moral support and patience has bared fruit through completion of this Thesis.

**DOLLY SOOD**

**ROLL NO. 300804005**

**DATE: 15/07/2010**

**Place: Thaper university patiala**

*Dedicated*  
*to*  
*my family*

## *ABSTRACT*

The present work deals with the theoretical study of Transverse flow, which develops because of different particles deflected sideward from the hot and dense region formed by the overlap of projectile and target nuclei. The study of transverse flow provides valuable data on the nuclear equation of state and isospin dependent N-N cross section. Study of dependence of transverse flow on beam energies, mass number, isospin and impact parameter have revealed quite interesting physics about the properties and origin of collective flow. At intermediate energies, the transverse flow disappears at certain incident energy, termed as balance energy  $E_{bal}$ . This phenomenon has been well established by many experiments during last decade. Simultaneously, much theoretical work has been devoted to understand the mechanism responsible for disappearance of transverse flow at balance energy and the isospin dependence of balance energy for  ${}_{26}\text{Fe}^{58}+{}_{26}\text{Fe}^{58}$  and  ${}_{28}\text{Ni}^{58}+{}_{28}\text{Ni}^{58}$  systems at different energies and different impact parameters. Here we have used isospin-dependent quantum molecular dynamical model (IQMD) for the present study.

# TABLE OF CONTENTS

# PAGE NO.

Certificate.....	1
Acknowledgement.....	2
Abstract.....	4
Table of contents.....	6
List of figures.....	7

## CHAPTER -1 INTRODUCTION

1.1 Heavy ion collision.....	(1)
1.2 Flow.....	(2)
1.3 Collectiveflow.....	(5)
1.4 Balanceenergy.....	(7)
1.5 Isospin symmetry.....	(8)
1.6 Experimental scenario.....	(9)
1.7 Theoretical methods.....	(10)
1.8 References.....	(13)

## CHAPTER – 2 METHODOLOGIES

2.1 Introduction.....	(15)
2.2 IBUU Model.....	(15)
2.3 IQMD Model.....	(19)
2.4 Cluster analysis.....	(22)
2.5 References.....	(23)

### **CHAPTER – 3      PHASE SPACE ANALYSIS**

3.1	Introduction.....	(24)
3.2	Snapshots of phase space.....	(24)
3.3	The Time Evolution.....	(29)
3.4	References.....	(33)

### **CHAPTER – 4      TRANSVERSE FLOWS**

4.1	Introduction.....	(34)
4.2	Directed flow.....	(34)
4.3	Difference in balance energies of symmetric system.....	(35)
4.4	Results and Discussion.....	(37)
4.5	References.....	(44)

### **CHAPTER -5      SUMMARY**

## LIST OF FIGURES

- Fig. 1.1** Shows situation before collision and after collision.
- Fig. 1.2** Display of the in-plane bounce off caused by compression and the squeeze out.
- Fig. 1.3** Shows bounce and squeeze out that occur in reaction plane.
- Fig. 1.4** Shows nucleus of an atom contains many nucleons (protons and neutrons). The nucleons are made up of quarks and gluons.
- Fig. 1.5** Phase diagram of nuclear matter.
- Fig. 3.1** A projection of spacial distribution of nucleons into ( X – Z ) & ( X – Y ) planes.
- Fig. 3.2** Same as fig.3.1 but in momentum space.
- Fig. 3.3** A projection of special and momentum space into ( X – Z ) and ( P<sub>x</sub> – P<sub>z</sub> ) planes.
- Fig. 3.4** The evolution of mean density and rate of nucleon-nucleon collisions as a function of time.
- Fig. 3.5.** Plot of rate of collisions as a function of time for different systems.
- Fig. 4.1.** Directed flow.
- Fig. 4.2** Plots of averaged P<sub>x</sub>/A as a function of Y<sub>c.m</sub>/Y<sub>beam</sub> for (<sup>28</sup>Ni<sup>58</sup>+<sup>28</sup>Ni<sup>58</sup>) system with σ=80% of free cross section.
- Fig. 4.3** Same as fig.4.2 but for <sup>26</sup>Fe<sup>58</sup>+<sup>26</sup>Fe<sup>58</sup> system.
- Fig. 4.4** The Time evolution of <P<sub>x</sub>dir> for <sup>28</sup>Ni<sup>58</sup>+<sup>28</sup>Ni<sup>58</sup> system.
- Fig. 4.5** Same as fig.4.2 but for <sup>26</sup>Fe<sup>58</sup>+<sup>26</sup>Fe<sup>58</sup> system.
- Fig. 4.6** Shows <P<sub>x</sub>dir > as a function of incident energy for <sup>26</sup>Fe<sup>58</sup>+<sup>26</sup>Fe<sup>58</sup> and <sup>28</sup>Ni<sup>58</sup>+<sup>28</sup>Ni<sup>58</sup>.
- Fig. 4.7.** Plot of balance energies as a function of impact parameter for <sup>26</sup>Fe<sup>58</sup>+<sup>26</sup>Fe<sup>58</sup> and <sup>28</sup>Ni<sup>58</sup>+<sup>28</sup>Ni<sup>58</sup>.

# CHAPTER1

## INTRODUCTION

### 1.1 Heavy ion collisions

The study of heavy ion collisions is a rapidly expanding subject. The term “heavy ion” is used for the nuclei massive than helium nucleus. The branch of Physics which deals with the phenomenon, when two heavy nuclei brought into contact, such that nuclear forces holding the protons and neutrons within the one nucleus are felt by the other nucleus, is called heavy ion physics. There are number of applications of heavy ion collisions in the field of science and technology.

Heavy ion physics has attracted much attention during last three decades. The behavior of heavy nucleus under extreme conditions such as temperature, density, angular momentum, pressure is a very important aspect of heavy ion physics. A large no. of accelerators have been developed to study these heavy ion reactions. The energy of accelerated heavy ions classified into following three categories:

- 1) Low ( $E < 10A$  MeV)
- 2) Intermediate ( $10A$  MeV to  $2A$  GeV)
- 3) High (more than  $2A$  GeV)

Heavy ion physics has been differentiated in 4 major branches on the basis of temperature and pressure.

- One of the branch discuss about deconfinement and quark-gluon plasma.
- Second branch deals with study of  $\gamma$ -ray spectroscopy.
- The third branch led to the study of nuclear collectivity through giant resonances and lastly, the branch that deals with the study of intermediate energy heavy ion collisions. In last two decades, a lot of efforts have been made experimentally as well as theoretically to understand the nuclear physics at intermediate energies ( $10A$  MeV and  $2A$  GeV).

The main interest of studying low energy heavy ion interactions is to look for low density phenomena. Here the colliding nuclei cannot compress each other. It gives unique possibility of studying fusion-fission reactions [26], cluster radioactivity [27], formation of super heavy elements, the possibilities of synthesis of super heavy elements through neutron rich beams, halo nuclei [1] etc. The reaction cross section at low energy compares of three types i.e., the fusion, quasi-elastic and deep inelastic scattering.

Naturally all these processes depend on the projectile-target combinations, incident energy and on angular momentum. The symmetric and asymmetric reactions were studied at low energy, and they were found to emit cluster. This branch (cluster radioactivity) has been studied quite extensively in last year's [1].

Heavy ion collisions (HIC) at intermediate and high energies provide a possibility for studying the properties of nuclear matter in conditions vastly different from that in normal nuclei, such as high density, high temperature and excitation as well as large differences in proton neutron numbers [2]. The nuclear equation of state (EOS) can be researched via liquid gas transition, multifragmentation and collective flow, such as directed and elliptic flow produced in heavy ion collisions. Such knowledge is not only of interest in nuclear physics but is also useful in understanding astrophysical phenomenon such as evolution of early universe. One observable that has extensively used for extracting nuclear (EOS) from heavy ion collisions at intermediate and high energies is the collective flow.

## **1.2 FLOW**

For the determination of the equation of state (EOS), the relationship between pressure and volume for nuclear matter, is an important objective of nuclear physics. The information about the equation of state can be extracted from the collective flow of nuclear matter deflected sideways from the hot and dense region formed by the overlap of projectile and target nuclei. The schematic diagram below illustrates the nuclear matter distributions for the projectile and target nuclei before the collision (on the left) and a

sidewards deflection of the nuclear matter after the collision (on the right) which is frequently termed "sidewards collective flow" or directed flow.

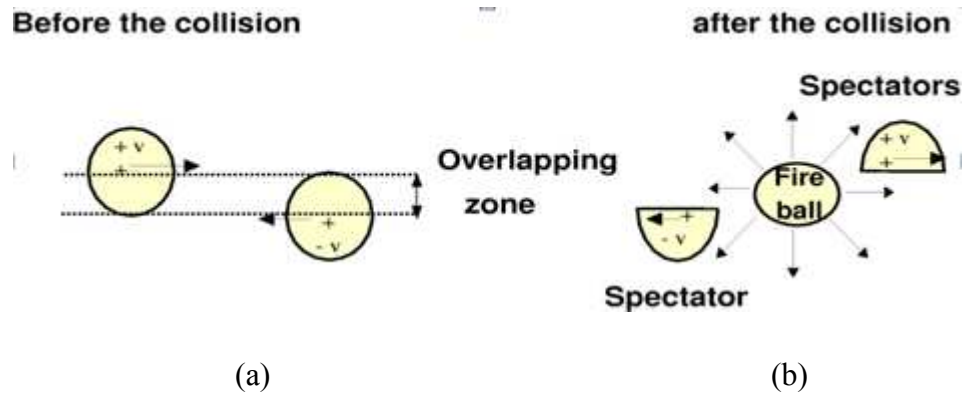


Fig.1.1 (a) and (b) shows situation before collision and after collision

When two nuclei approach each other, they feel attractive potential causing the collective transverse momentum in the direction opposite to the impact parameter. As soon as colliding nuclei overlap, particles with very large momenta are positioned closely in the configuration space due to which the potential becomes repulsive and accelerates the particles in the transverse direction. Whereas outside the overlap zone, there are either projectile or target nucleons. Therefore, the potential is still attractive. As a result of this, there is a strong potential gradient perpendicular to the beam direction in the reaction plane (where reaction plane is defined by the impact parameter  $b$  and the beam axis  $z$ ) due to which an appreciable amount of the transverse momentum is transferred to the detected particles along the direction of impact parameter. This transverse momentum causes the system to expand radially, thus decreasing the density. A pictorial display of in-plane bounce off and squeeze out is presented in Fig.1.2.

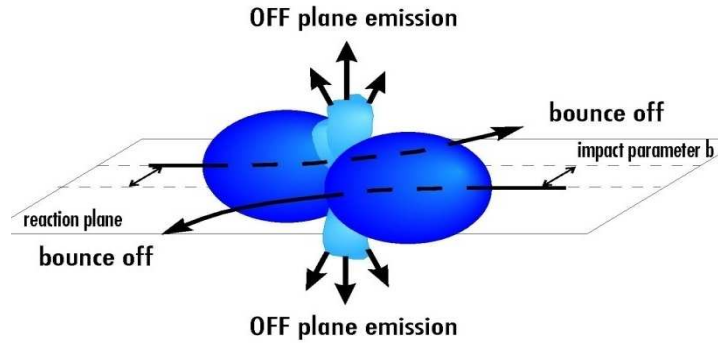


Figure 1.2: Display of the in-plane bounce off caused by compression and the squeeze out, the enhanced emission of light particles perpendicular to the plane close to midrapidity.

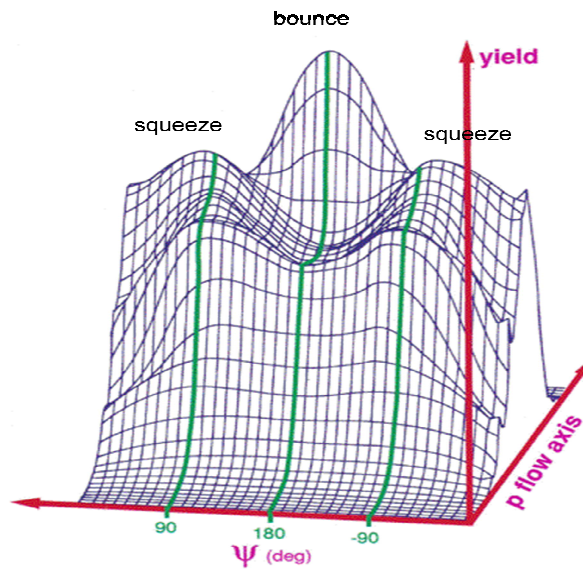


Figure 1.3 shows bounce and squeeze out that occur in reaction plane

If two nuclei collide and a high density zone is built up, interactions of the compressed zone may become rather strong and initiate collective effects. Two major effects can be found which have been (qualitatively) predicted by hydrodynamical calculations and have been confirmed by experiments:

1. A deflection of the projectile and target remnants (which do not belong to the overlap region of the two nuclei and thus are called spectators) by the high density region

(the so-called participants). These particles get a sideward kick which is called the *bounce-off*.

2. Particles of the high density region escape from the compressed zone. They are *squeezed-out* perpendicular to the reaction plane, i.e. in that direction where no remnants of the nuclei are covering the compression region.

Flow is caused by the short range nuclear repulsion and its strength decreases with decreasing energy. At very low energy the attractive part of the nuclear potential becomes more important and the direction of flow is reversed. This disappearance of flow can be observed experimentally [3]. The energy at which flow is zero is called balance energy. It can be determined very precisely and is quite independent of detector biases. The FOPI collaboration has emphasized the importance of the fragments in their systematic analysis of directed fragment flow.

### **1.3 Collective flow**

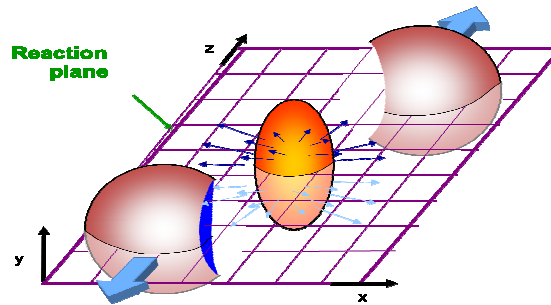
Nuclear collective flow is a kind of collective phenomena found in intermediate and high energy heavy ion collisions and is the measure of transverse motion imparted to particles and fragments during the collision of two nuclei. The development of collective flow is closely related to the pressure build up during the compression stage of reaction and gives us information about pressure and particle density relation (i.e EoS). Study of dependence of directed flow, elliptic flow and different fragment flows on beam energies, mass number, isospin and impact parameter have revealed quite interesting physics about the properties and origin of collective flow.

In recent years, much emphasis has been placed on the study of collective flow and several groups have already performed experiments to study its disappearance at balance energy, which is closely related to nuclear EOS.

Mainly there are three types of flow elliptical flow, transverse flow and radial flow.

### **(a) Elliptic flow**

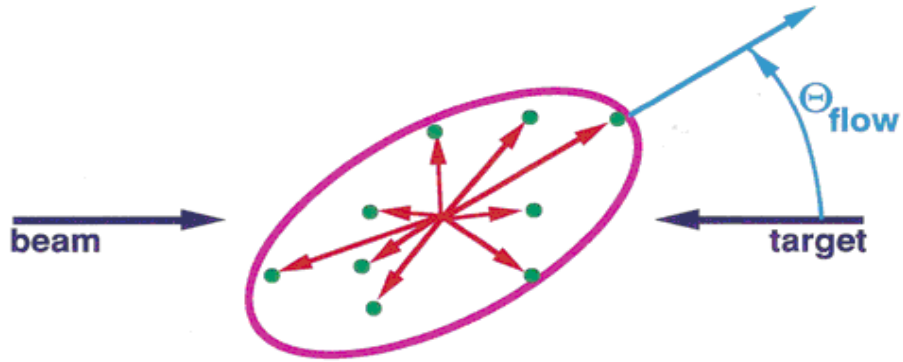
Elliptic flow develops because of the almond shape of the overlapping region in a heavy ion collision. The elliptic flow is expected to be larger in peripheral collisions. The study of directed and elliptic flow provides valuable data on the nuclear equation of state and isospin dependent N-N cross section.



(a) Elliptical flow

### **(b) Transverse flow**

The phenomenon of different fragments or different particles deflected sideward from the hot and dense region formed by the overlap of projectile and target nuclei is called transverse flow or directed flow, which was used to extract nuclear EOS frequently. Directed flow effects mostly particles at forward and backward rapidities which (at energies above a few hundred MeV/nucleon) are deflected away from the beam direction by pressure built up between the colliding nuclei during the time of their mutual overlap. Thus effected particles quickly leaves the central region where this transverse pressure force acts, the finally observed directed transverse flow pattern is established very early in the collision. This transverse flow has property to become zero at particular incident energy known as balance energy or energy of vanishing flow.



(b) Transverse flow

### **(c) Radial flow**

Radial flow is generated by the pressure gradient between the interior of collision fireball and the external vacuum. This force persists throughout the fireball expansion until freeze-out.



(C) Radial flow

### **1.4 Balance energy**

In particular, the excitation function of transverse flow from low to ultra-relativistic energies has been found especially interesting on high energy side. At intermediate energies, the transverse flow disappears at certain incident energy, termed as balance energy. This phenomenon has been well established by many experiments during last decade. Simultaneously, much theoretical work has been devoted to understand the mechanism responsible for disappearance of transverse flow at balance energy. It has

been suggested that at balance energies the attractive scattering dominate at energies around 10 MeV/neuclon balances the repulsive interactions dominate at energies around 400MeV/ neuclon. Study of either the directed flow or the elliptical flow has been studied separately in the likewise, but combined researches considering isospin dependence for asymmetric systems are still a few [4].

## **1.5 Isospin symmetry**

In quantum mechanics when the Hamiltonian has symmetry, that symmetry manifests itself through a set of states that have the same energy that is the states are degenerate. In particle physics the near mass degeneracy of neutron and proton points to an approximate symmetry of Hamiltonian describing the strong interactions. The neutron does have slightly higher mass due to isospin breaking. This is due to the difference in the masses of the up and down quarks and the effects of electromagnetic interaction. However the appearance of approximate symmetry is still useful, since the small breaking can be described by perturbation theory which gives rise to slight differences between near degenerate states [5].

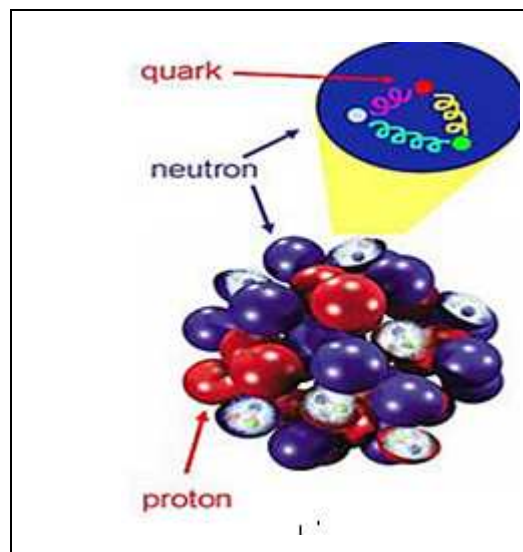


Figure1.4: shows nucleus of an atom contains many nucleons (protons and neutrons). The nucleons are made up of quarks and gluons.

As our main focus is on to the isospin dependence of the balance energy. In the proceeding section, the experimental as well as theoretical findings of balance energy are discussed in detail.

## **1.6 Experimental scenario**

The first experiments at Berkeley served mainly to get the experimentalists and theoreticians aware of the problems and pitfalls of the way from intermediate energy heavy ion collisions to nuclear matter equation of state. Latter on several accelerators were built at Michigan state university (USA), GANIL(France), GSI (Germany), relativistic energy heavy ion collider (RHIC) and superconducting supercollider(SSC) at BNL(USA). The heavy ion synchrotron (SIS) accelerator at GSI is specially designed to study the heavy ion reactions at intermediate energies. These measurements provide a complete analysis of flow over wide range of mass, incident energy and colliding geometry i.e. impact parameter.

The collective flow was measured for the first time by the Berkeley group for  $^{40}\text{Ca}+^{40}\text{Ca}$  and  $\text{Nb}^{93}+\text{Nb}^{93}$  reactions at 400MeV/nucleon using plastic ball /plastic wall detector at BEVALAC [6]

Several methods have been used to measure the collective transverse in plane flow. The first attempt to measure the balance energy in this flow was made by the MSU group [8]. The balance energy was measured for  $^{139}\text{La}+^{139}\text{La}$  reaction by Kropf et al. [8]. Latter on balance energy was measured for  $^{40}\text{Ar}+^{51}\text{V}$  [31],  $^{93}\text{Nb}+^{93}\text{Nb}$  [8],  $^{36}\text{Ar}+^{27}\text{Al}$  [13],  $^{64}\text{Zn}+^{48}\text{Ti}$  [13],  $^{64}\text{Zn}+^{58}\text{Ni}$  [13],  $^{40}\text{Ar}+^{58}\text{Ni}$  [32],  $^{58}\text{Ni}+^{58}\text{Ni}$  [15] and  $^{129}\text{Xe}+\text{Sn}$  [32] reactions. The very recent and accurate measurement of balance energy in  $^{197}\text{Au}+^{197}\text{Au}$  [28-32] has generated a renewed interest in the field [33]. Interestingly, most of the reported reactions are symmetric in nature. It should be kept in mind that the reaction dynamics depends also on the asymmetry of the reaction [34]. All the above mentioned measurements were for the central collisions only. The above findings reveal the measurements of balance energy in more than 15 systems ranging from very light to

heavy nuclei. As a result a power law behavior ( $\propto A^T$ ) has been reported for balance energy. The balance energy was found to be sensitive for both nuclear matter equation of state and as well as in medium nucleon-nucleon cross section [9, 14]. The INDRA collaboration at GANIL studied for the first time  $E_{\text{bal}}$  as a function of impact parameter for  $^{40}\text{Ar} + ^{27}\text{Al}$  reaction [10]. The experiments are carried out at national superconducting cyclotron laboratory (NSCL) using heavy ion beam from the K1200 cyclotron. After four years of operation strong experimental evidence has been accumulated that at RHIC energies, a new state of matter is indeed created which is quantitatively different from hadron gas. Later on impact parameter dependence of balance energy was studied for  $^{64}\text{Zn} + ^{27}\text{Al}$  [11],  $^{40}\text{Ar} + ^{45}\text{Sc}$  [12, 16],  $^{58}\text{Ni} + ^{58}\text{Ni}$  [16],  $^{86}\text{Kr} + ^{93}\text{Nb}$  [16] and  $^{197}\text{Au} + ^{197}\text{Au}$  reactions [16].

It was found that the balance energy increases approximately linearly as function of impact parameter [10-12, 16]. Recently, collective transverse flow has been observed experimentally to depend on isospin of the colliding system, confirming the predictions of BUU model which incorporates the isospin dependent mean field and in medium nucleon-nucleon cross-section. Various theoretical attempts have been made to understand the vanishing of nuclear transverse in-plane flow. Most of these are however, using the BUU model. Some attempts are also reported in literature where quantum molecular dynamical (QMD) model was used. Different theoretical attempts considered either a stiff or soft equation of state along with a variety of nucleon-nucleon cross-sections.

## **1.7 Theoretical methods**

As two heavy nuclei approach each other in a collision, they form a highly-correlated strongly-interacting finite quantum system. As they collide and the beam energy is distributed, the participant nucleons reach higher energy levels where the Pauli principle is less restrictive on the energy transfer. At this point the nuclear Fermi-gas begins to resemble a more classical one, and thus one is allowed to speak of temperature and phase transitions in the classical sense. After presumed phase transition takes place, the system

expands and disassembles into clusters (liquid droplets and gaseous particles), which continue de-exciting by further fission and photon particle emission.

This transition from a quantum regime to a more classical one, and back again to the quantum world, makes heavy-ion reactions practically impossible to track analytically. Apart from being a many-body system (for which no exact solutions exist), the reaction dynamics are highly out-of-equilibrium and required the use of quantum kinetic theory which does not exist yet. Fortunately, since the collision can be divided into, say, three stages, collision/compression, expansion/breakup, and cooling, computational models with some predictive power have been devised.

Theoretically, several models have been developed which make the situation more complicated. The key point to remember is that heavy-ion collision involves very complicated non-equilibrium physics, therefore, its numerical modeling is not straight forward. Due to lack of free space at low incident energies about 98% of the attempted collisions are blocked. The whole dynamics at low energies is governed by the mean field or by the two body and three body interactions. In contrary the availability of large free phase space at relativistic energies ( $>2$  GeV) makes Pauli principle's role quite small (roughly 4% collisions are blocked) and hence the dynamics of reaction is governed by the Cascade picture. On the other hand, both Cascade and mean field emerges at intermediate energies.

These models can be broadly divided into dynamical and statistical models, with some hybrid approaches linking these two extremes.

**Time Dependent Hartree-Fock (TDHF):** The conventional theories like time dependent Hartree-Fock (TDHF) [17] or its semi-classical version the so called Vlasov equation (in phase-space) are suitable approaches at low energies where the nucleon-nucleon collisions are negligible. A suitable (and reasonable) approach for intermediate energy heavy-ion physics should treat the nucleon nucleon collisions and mean field on equal footing. Some attempts were made in the literature to extend the TDHF to take care of the residual nucleon-nucleon (NN) interactions which are

responsible for two body collisions (this was dubbed as ETDHF)[18]. However due to complications, this theory could not be used for large scale investigations.

**Boltzmann-Uehling-Uhlenbeck:** Increasing in complexity from a single-particle description mean fields can be introduced to modulate the overall behavior of nucleons. In the BUU model, the heavy ion collision is described by the temporal evolution of the one-body density within mean field. This mean field is usually taken as that produced by the motion of the nucleons averaged over an ensemble of configurations.

Other related approaches are the Vlasov-Uehling-Uhlenbeck and the Boltzmann-Langevin methods. The two body collisions are treated in a rather phenomenological way by employing the Monte-Carlo technique. As all these techniques use only a mean field ignoring higher order correlations, these approaches, along with BUU, are not able to explore cluster formation. Refined models introduce mean field fluctuations to artificially induce clustering, or are used in hybrid models to add an ad hoc fragmentation.

**Molecular dynamics:** The classical molecular dynamics (MD) [19] approach is capable of treating both compression and fragment formation. The molecular dynamics predicts the collective flow in a qualitative agreement with the data. It incorporates the complete classical N-body dynamics which is necessary to describe the formation of fragments. Naturally, the simple classical molecular dynamics needs refinement which should also include quantum features. In nuclear physics, the key problem in MD methods lies in the treatment of the Pauli principle. Nucleons are fermions and it is difficult to speak of nuclei without the Pauli principle. This question is simply overlooked in strictly classical calculations. MD methods with Pauli principle address this question but with disputable success.

**Quantum Molecular Dynamics:** The QMD model [5] attempts to manipulate a many-body wave function to introduce the correlations needed for cluster formation. Taking the wave function as a product of coherent states and using momentum

dependent interactions with Pauli blocking, the model evolves a set of test particles through the temporal evolution of the reaction.

In past decade, several refinements and improvements were made over original QMD. The QMD model takes into account the Pauli principle, but through two-body collisions, which is somewhat contrary to MD picture. In view of the difficulties encountered with taking the Pauli principle in classical MD methods properly into account, a new class of approaches was developed in the beginning of the 1990s, the so called Fermionic Molecular Dynamics (FMD) [20,21] and AMD for antisymmetrized molecular dynamics[23,24]. The serious numerical problems have restricted the use of FMD and AMD approaches to light nuclei.

These new versions were named as IQMD (Isospin-QMD), GQMD (G-matrix-QMD [22, 23]. It is worth to mention that the Intra nuclear Cascade model (INC) developed by Cugnon et. Al. [24], is one of the pioneering models in the field and has acted as a guideline for the development of the field.

**Isospin dependent Quantum Molecular Dynamics:** IQMD model [25] in heavy ion collisions is used for studying the isospin effects on nuclear transverse collective flow, on nuclear radial flow and nuclear fragmentation.

The dynamics in the formation of the transient state is mainly governed by three components, namely, the mean field, two body collisions, and Pauli blocking. For an isospin dependent reaction dynamics algorithm it is essential that all the three components should reasonably include isospin degrees of freedom. In addition, it is also important that, in initialization of projectile and target nuclei, the samples of neutrons and protons in phase space should be treated separately since there exists a large difference between neutron and proton density distributions for nuclei. IQMD model is developed just on above basis. It has been shown that the IQMD can be used with large success for studying the effects of isospin in heavy ion collisions at intermediate energies. The detailed analysis of IQMD model is studied in the next chapter.

## **1.8 Refferences:**

- [1] R.K. Puri, P. Chattopadhyay and R. K. Gupta, Phys. Rev. C **43**, 315 (1991); R. K. Puri and R. K. Gupta, J. Phys. G 17, 1933 (1991); M. K. Sharma, H. Kumar, R. K. Puri and R. K. Gupta, Phys. Rev. C **56**, 1175 (1997).
- [2] W.Cassing, V.Metag, U. Mosel and K.Naiita, Phys. Rep. **188** 363 (1990).
- [3] D. Krofcheck, W. Bauer, G.M. Crawley, C. Djalali, S. Howden, A. Vander Molen, G.D.Westfall, R.S. Tickle, and C. Gale, Phys. Rev. Lett. **63**, 2028 (1989).
- [4] J. Lukasik et al. Phys. Rev C 55,1906 (1997).
- [5] J. Aichelin, Phys. Rep. **202**, 233 (1991).
- [6] H.A Gustafsson et al. Phys.Rev.lett. **52**,1590(1984).
- [7] G.D. Westfall et al. Phys.Rev.Lett.**71**, 1986(1993)
- [8] J.J Molitoris and H.Stocker,Phys. lett.B **162**,47 (1985);V.de la Mota et.al. Phys.Rev.C 46,677(1992);G.F. Bertsch, W.G. Lynch,and M.B.Tsang, Phys. lett. B 189,384(1987), D.Krofcheck et al.,Phys. Rev. Lett.63, 2028(1989);J. Peter, Nucl. Phys. A545, 173(1992).
- [9] D.Krofcheck et al.,Phys.Rev.C **46**,1416(1992).
- [10] J.P Sullivan et al.,Phys.Lett.B **249**,8(1990).
- [11] Z.Y.He et al.,Nucl.Phys.A **598**,248(1996).
- [12] R.Pak et al., Phys.Rev.C 54, 2457(1996); ibid Phys. Rev.C **53**, R1469 (1996).
- [13]A. Buta et.al., Nucl.Phys.A 584, 397 (1995); J.C. Angelique et al.,Nucl.Phys **614**, 261(1997).
- [14] C.A. Ogilvie et al., Phys.Rev. C **42**,R 10 (1990).
- [15] D.Cussol et al., Phys. Rev. C **65**, 044604(2002).

- [16] D.J. Magestro, W. Burer, and G.D. Westfall, Phys. Rev. C **62**, 041603(R) (2000) G.D. Westfall, Nucl. Phys. A.
- [17] H. Stoecker and W. Greiner, Phys. Rep. **137**, 277 (1986).
- [18] E. Suraud, Ch. Gregoire and B. Tamain, Prog. Part. Nucl. Phys. **23**, 357 (1989).
- [19] G. Peilert, A. Rosenhauer, J. Aichelen, H. Stoecker and W. Geiner, Mod. Phys. Lett. A **3**, 459 (1998).
- [20] E. Lehmann, R. K. Puri, A. Faessler, G. Batko and S.W. Huang, Phys. Rev. C **51**, 2113 (1995).
- [21] H. Feldmeir, J. Schnack, Proc. Int. Workshop on Dyn. Features of Nuclei, Spain (1993) World Scientific: H. Feldmeir, J. Schnack, Nucl. Phys. A **583**, 347c (1995); H. Feldmeir, K. Bieler, J. Schnack, Nucl. Phys. A **586**, 493 (1995).
- [22] A. Bohnet, N. Ohtsuka, J. Aichelin, R. Linden and A. Faessler, Nucl. Phys. A **494**, 349 (1989).
- [23] M. Trefz, A. Faessler and W. H. Dickhoff, Nucl. Phys. A **443**, 499 (1985).
- [24] J. Cugnon and C. Hartnack and J. Aichelin, Phys. Rev. C **54** (1993).
- [25] Ch. Hartnack, Rajeev K. Puri, J. Aichelin et al., Phys. J. A **1151**, **169** (1998)
- [26] N.K. Dhiman, Rajeev K. Puri Acta Physica B, **38** (2007).
- [27] T.R. Routray, Jagajjaya Nayak and D.N. Basu Nucl. Phys. A **826**:223-229 (2009).
- [28] D. Cussol et al., Phys. Rev. C **65**, 044604 (2002).
- [29] E. Lehmann, A. Faessler, J. Zipprich, R.K. Puri, et al., Phys. A **355**, 55 (1996).
- [30] S. Kumar, M.K. Sharma, R.K. Puri, Phys. Rev. C **69**, 054612 (2004).
- [31] A. D. Sood and R. K. Puri, Phys. Lett. B **594**, 260 (2004).

[32] G. F. Bertsch and S. Das Gupta, Phys. Rep. 160,189 (1988).

[33] H. Huber and J. Aichelin, Nucl. Phys. A573, 587(1994).

[34] J. Cugnon, T. Mizutani, and J. Vandermeulen, Nucl. Phys. A352, 505 (1981).

### 2.1 Introduction

Recently, the isospin dependence of collective flow has become an interesting subject of experimental and theoretical investigations. It is understood in principle but is demonstrated in series of microscopic model calculations such as isospin –dependent quantum molecular dynamic model (IQMD) and Boltzmann-Uehling-Uhlenbeck (IBUU) model.

The isospin dependence of collective flow has been studied by Li et. al. and Zheng et al in terms of isospin –dependent Boltzmann-Uhlenbeck (IBUU) model in which the proton and neutron densities were calculated from non relativistic mean-field (RMF) theory.

### 2.2 Isospin - Boltzmann – Uehling – Uhenbeck (IBUU) Model

The IBUU model treats protons and neutrons explicitly and includes an asymmetry term in nuclear mean –field potential and different scattering cross sections for proton and neutrons and includes an asymmetry term in the nuclear mean-field potential and a different scattering cross section for protons and neutrons. The model has been used recently to explain successfully several phenomena in heavy-ion collisions at intermediate energies [1]. Isospin – dependent BUU model solves the transport equation:

$$\partial_1 f_1 + \frac{\vec{p}}{E} \vec{\nabla}_r f_1 - \vec{\nabla}_r U \vec{\nabla}_p f_1 = \int \frac{d^3 p_1' d^3 p_2 d^3 p_2'}{(2\pi)^3} \sigma_{12} v_{12} (2\pi)^3 \delta^3(\vec{p}_1 + \vec{p}_2 - \vec{p}_1' - \vec{p}_2') \times \left\{ f_1' f_2' (1 - f_1)(1 - f_2) - f_1 f_2 (1 - f_1')(1 - f_2') \right\}$$

The isospin dependence comes into the model through both the elementary nucleon-nucleon cross sections  $\sigma_{12}$  and the nuclear mean field  $U$ . Here we use the experimental

nucleon-nucleon cross sections with explicit isospin dependence. The isospin resides in the fact that the cross section of neutron-proton collisions is about three times that of neutron-neutron or proton-proton collisions. We keep in mind, however, that in-medium cross sections and their isospin dependence might be strongly density dependent. The nuclear mean field  $U$  including the Coulomb and isospin symmetry terms is parametrized as:

$$U(\rho, \tau_z) = a \left( \frac{\rho}{\rho_0} \right) + b \left( \frac{\rho}{\rho_0} \right)^\sigma + (1 - \tau_z) V_C + C \frac{\rho_n - \rho_p}{\rho_0} \tau_z$$

In the above,  $\rho_0$  is the normal nuclear matter density;  $\rho$ ,  $\rho_n$ , and  $\rho_p$  are the nucleon, neutron, and proton densities, respectively;  $\tau_z$  equals 1 or -1 for neutrons or protons, respectively; and  $V_C$  is the Coulomb potential.

### **Limitations of IBUU Model**

- The IBUU and BUU model cannot describe the observable of two body relevancy such as the fragment flow since it is a one body transport model and does not contain many body correlations these phenomena reflects a strong nuclear relevancy and large physical fluctuation in a low density nuclear system exists.
- Meanwhile the IBUU model cannot describe the phenomena such as cluster formation and multifragmentation produced in heavy ion collisions.

But IBUU can describe the behavior of collective flow such as collective rotation, and quantitatively and qualitatively explains the physical results.

### **2.3 Isospin Quantum molecular dynamics (IQMD)**

The IQMD model has been successfully used for the analysis of large number of observables and from low to high energies. It treats different charge states of nucleons, pions and deltas explicitly as inherited from Vlasov-Uehling Uhlenbeck (VUU) model [2, 3]. The isospin degree of freedom enters into the calculations via symmetry potential,

cross sections and coulomb interaction [4]. As it is developed from VUU model, so it's coding is independent of original QMD.

### **Initialization in IQMD**

In this model the nucleons are represented by the Gaussian-shaped density distributions. Here the centroids of the Gaussians in the nucleus are randomly distributed in a phase space sphere ( $r \leq R$  and  $P \leq P_F$ ) with  $R = 1.12A^{1/3}$  fermi corresponding to the ground state density  $\rho_0 = 0.17 \text{fm}^{-3}$ . The Fermi momentum depends on the ground state density. For  $\rho_0 = 0.17 \text{fm}^{-3}$  the value of  $P_F \approx 2.68 \text{MeV}/c$ . due to this collision the nucleons (where the local potential energy is low) are unbounded initially. As a result binding energy is low as compared to the Weizsacker mass formula; hence the initialized nuclei are less stable against spurious particle evaporation as compared to QMD model. Finally it should be noted that IQMD performs a Lorentz contraction of the nucleus coordinate distribution which is not present in QMD and also important for higher energies [5].

### **Interaction range**

Gaussian width is regarded as a description of the interaction range of a particle. Its influence disappears at infinite nuclear matter whereas for finite systems it plays an important role. It is denoted by  $L$ .

In IQMD the Gaussian width can be used as an optional input parameter. The system dependence of  $L$  in IQMD has been introduced in order to obtain maximum stability of the nucleonic density profiles. As an example for Au+Au a value of  $L = 8.66 \text{fm}^2$  is chosen, for Ca+Ca and lighter system  $L = 4.33 \text{fm}^2$ .

### **Propagation**

In isospin quantum molecular dynamical (IQMD) [6-7] model, the nuclei are represented by Gaussian shaped density distributions.

$$f_i(\vec{r}, \vec{p}, t) = \frac{1}{\pi^3 \hbar^3} \times e^{-\frac{(\vec{r} - \vec{r}_i(t))^2}{L}} \times e^{-\frac{(\vec{p} - \vec{p}(t))^2}{2\hbar^2}} \quad (1)$$

The nuclei which are successfully initialized are boosted towards each other with a proper centre of mass velocity using relativistic kinematics. The particles are propagated under the total interaction calculated by the Hamiltonian equations of motion

$$\frac{dr_i}{dt} = \frac{d\langle H \rangle}{dp_i}, \quad \frac{dp_i}{dt} = - \frac{d\langle H \rangle}{dr_i}$$

The total one nucleon Weigner density is, therefore, the sum of all nucleons. The expectation value of Hamiltonian

$$\langle H \rangle = \langle T \rangle + \langle V \rangle$$

$$\sum_i \frac{p_i^2}{2m_i} + \sum_i \sum_{j>i} \int f_i(\vec{r}, \vec{p}, t) V^{ij}(\vec{r}', \vec{r}) \times f_j(\vec{r}', \vec{p}', t) d\vec{r} d\vec{r}' d\vec{p} d\vec{p}' \quad (2)$$

The baryon-baryon potential  $V^{ij}$  consists of real part of Bruckner G-matrix which is supplemented by an effective Coulumb interaction acting between the charged particles. The former part can be parameterised in term of Skyrme type interaction to finite range Yukawa potential as well as momentum dependent contribution [8-10]. In addition, a symmetry potential between protons and neutrons corresponding to the Bethe-Weizsacker formula has been included. Therefore,  $V^{ij}$  consists of:

The potential in this equation is the sum of following specific elementary Potentials:

$$V^{ij} = G^{ij} + V_{Coul}^{ij}$$

$$V^{ij} = V_{loc}^{ij} + V_{Yuk}^{ij} + V_{Coul}^{ij} + V_{Sym}^{ij} + V_{Mdi}^{ij} \quad (3)$$

With local hard core repulsion

$$V_{loc}^{ij} = \sum_i \sum_{i>j} \mathbf{t}_1 \delta(\vec{r}_i - \vec{r}_j) + \sum_i \sum_{i>j} \sum_{k>j} \mathbf{t}_2 \delta(\vec{r}_i - \vec{r}_j) \delta(\vec{r}_i - \vec{r}_k) \quad (4)$$

The yukava long range term

$$V_{yuk}^{ij} = \sum_i \sum_{i>j} t_3 \frac{e \frac{|\vec{r}_i - \vec{r}_j|}{a}}{\frac{|\vec{r}_i - \vec{r}_j|^2}{a}} \quad (5)$$

The coulomb term with only a mean value for the nucleon charge because QMD does not know the isospin of particles,

IQMD parameters		
$t_3$	1.5	MeV
$t_4$	1.57	MeV
$t_5$	$5.10^{-4}$	$\text{MeV}^{-2}$
$t_6$	25	MeV
$a$	0.4	fm

Table 2.1: QMD and IQMD parameters used in equation (5) to (8)

The coulomb value with only mean value for the nuclear charge because QMD does not know the isospin of particles.

The momentum dependent interaction [9-10]

$$V_{mdi}^{ij} = \sum_i \sum_{i>j} t_4 \ln^2(1+t^5 ((\vec{p}_i - \vec{p}_j)^2)) \delta(\vec{r}_i - \vec{r}_j) \quad (6)$$

For the comparison with the experimental results an extension of the microscopic QMD model is used. The IQMD contains the isospin degrees of freedom and free pion propagation. The isospin treatment via a symmetry potential allows for distributions of protons and neutrons. The symmetry potential,

$$V_{sym}^{ij} = t_6 \frac{1}{\rho_0} T_i T_j \delta(\vec{r}_i - \vec{r}_j) \frac{1}{\rho_0} \quad (7)$$

With isospin quantum no  $T_i$  is an additional term to equation .If the particle is a proton  $T_i = 1$  and in case of neutron no  $T_i = -1$ . Furthermore equation changes to

$$V_{coul}^{ij} = \sum_i \sum_{j>i} \frac{z_i z_j e^2}{|\vec{r}_i - \vec{r}_j|} \quad (8)$$

with the explicit charges of particles. In IQMD pion creation and absorption are treated via resonances processes (pion production and pion absorption).

The parameters of the used version of IQMD are summerised here and in table 2.1.

Using IQMD model, we will study the directed flow of different fragments in the reaction of  ${}_{28}\text{Ni}^{58} + {}_{28}\text{Ni}^{58}$  and  ${}_{28}\text{Fe}^{58} + {}_{28}\text{Fe}^{58}$  systems. Meanwhile the role of impact parameter and the nuclear EOS will also study in next chapters. The IQMD model provides some information about both the collision dynamics and fragmentation process.

## **2.4 Cluster analysis:**

The minimum spanning tree method (MST) [10] is used in cluster analysis and track finding, if we consider tracks to be clusters of points. This method identifies two nucleons in a same fragment if their centroids are less than a distance  $d_{\min}$ . Before one can study the origin of fragments one has to identify the fragments.

$$|r_i - r_j| \leq d_{\min}$$

Where  $r_i$  and  $r_j$  are the special positions of both nucleons.

One simulates the reaction using IQMD. Then spatial distance of all nucleons is checked. A nucleon is part of a fragment if there is another one within a distance of  $r_{\min} = 4$  fm. Recently a new approach has been developed which defines the fragments in phase space. There nucleons can form fragment if the total energy/nucleon is below a minimum binding energy. Till today, this method is one of the most extensively used methods.

## **2.5 References:**

- [1] B. A. Li and S. J. Yennello, Phys. Rev. C **52**, R1746 (1995).
- [2] C. Hartnack. Ph.D Thesis, GSI-Report **93,5** (1993).
- [3] C. Hartnack, L. Zhuxia, L. Neise, G. Peilert, A. Rosenhauer, H. Sorge, J. Aichelin, H. Stocker and W. Greiner, Nucl. Phys. A **495** 303 (1989).
- [4] H. Kruse, B.V. Jacak, H. Stocker, Phys Rev. Lett. **54**, 289 (1995); J.J. Motalorias Phys Rev C **32**, 346(R).
- [5] Ch. Hartnack, Rajiv K Puri, J Aichelin, J Konopka, S.A.Bass, H.Stocker, W. Greiner, Eur Phys. J. A **1 151**, 169 (1998).
- [6] Sakshi Gautam, Rajiv Chugh , Aman D.Sood ,Rajeev K.Puri,Ch. Hartnack and J. Achelin.Nucl-th **1443**, 2(2010).
- [7] J. Aichelin, Phys. Rev. **202**, 233 (1991).
- [8] P. B. Gossiaux and J. Aichelin, Phys. Rev. C **56**, 2009.
- [9] Suneel kumar, Sanjeev kumar and Rajiv. K. Puri. Phys. Rev. C **81**, 014601 (2010).
- [10] S. Kumar and R. K. Puri, Phys. Rev. C **58**, 320 (1998).

## CHAPTER – 3

### PHASE SPACE ANALYSIS

---

#### 3.1 Introduction

In the previous chapters, we studied the detail of heavy ion reactions. At low incident energies, fusion is more probable whereas at intermediate energies multifragmentation dominates. At high incident energies, a clear evaporation is seen. In the following sections, we will present phase space analysis of heavy ion collisions and the rate of nucleon-nucleon collisions as a function of time.

#### 3.2 Snap – shots of the phase space

Here we will study the time evolution of heavy ion reaction. One way to look at phase space is to study the phase – space in X–Y and X–Z planes. In figure 3.1. and 3.2, we display the phase – space of  ${}_{28}\text{Ni}^{58}+{}_{28}\text{Ni}^{58}$  reaction at  $E = 65$  MeV/nucleon and  $\hat{b} = \left( \frac{b}{b_{max}} \right) = 0.4$  at different times. The figure 3.1 is representing the coordinate phase-space analysis, while figure 3.2 the momentum-space respectively. Here both front and side views are displayed. The front( X-Z ) and side views ( X-Y ) are quite different pictures for a non-central collision. Two nuclei are far apart in ( X–Z ) plane as compared to (X–Y) plane.

During the initial stages of the reaction, projectile and target are well separated both in coordinate and momentum space and as a result, whole of the matter is in the form of spectator matter only. This is called the initial phase. As the nuclei overlap, the density increases, that leads to more and more collisions that changes the interacting matter from spectator to participant one. At impact parameter  $\hat{b} = \left( \frac{b}{b_{max}} \right) = 0.4$ , some of the nucleons (spectators) never undergo a collision with nucleons of the collision partner. These nucleons experience only the (distorted) mean field of their parent nuclei and propagate with little deflection. If we increase the impact parameter, we will notice a reduced intensity of participant matter.

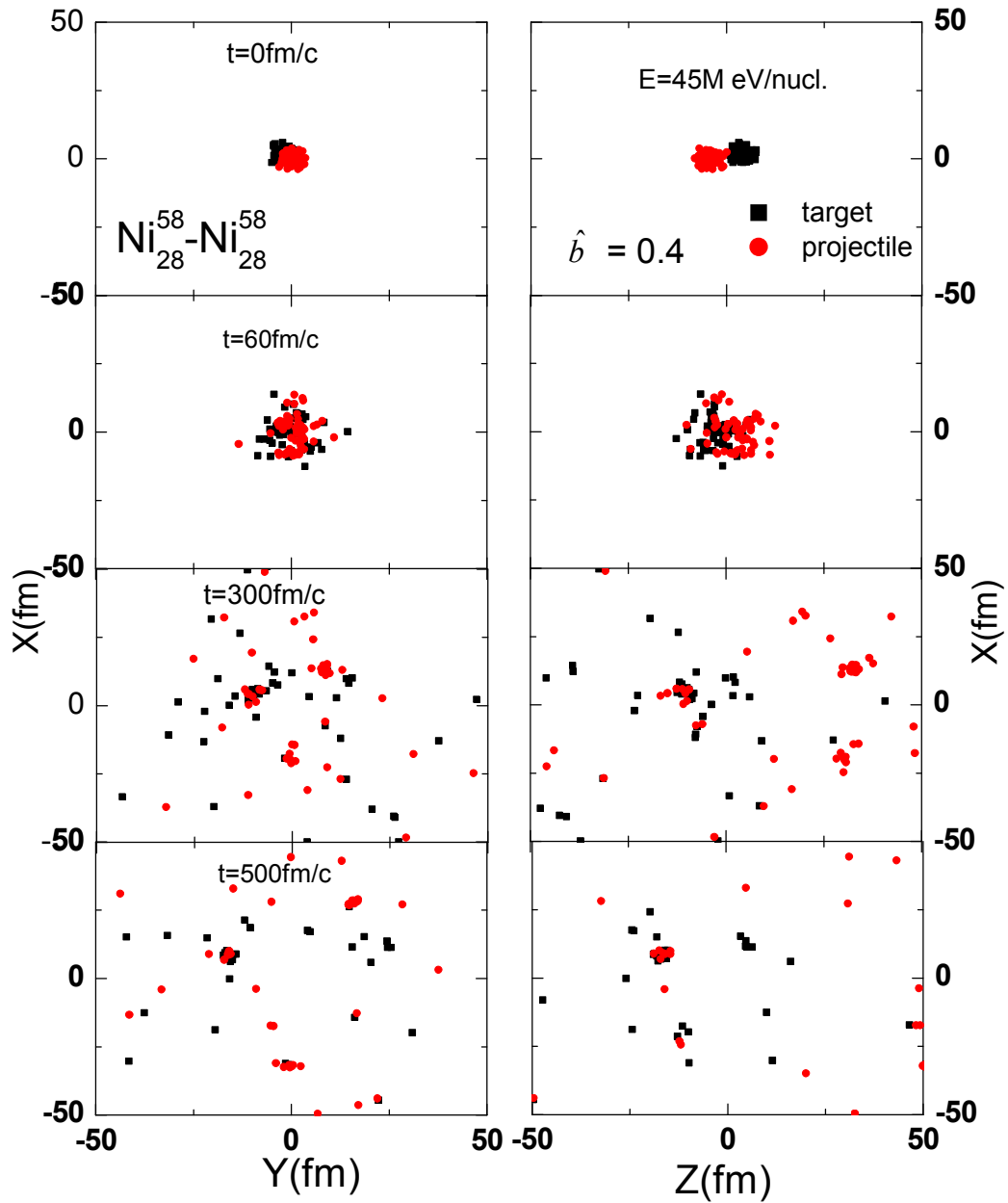


Figure 3.1: The evolution of the reaction  ${}_{28}\text{Ni}^{58} + {}_{28}\text{Ni}^{58}$  at  $\hat{b} = 0.4$  and incident energy of 45 MeV/nucleon. This plot is a projection of spatial space into  $(X$ - $Y)$  &  $(X$ - $Z)$  planes.

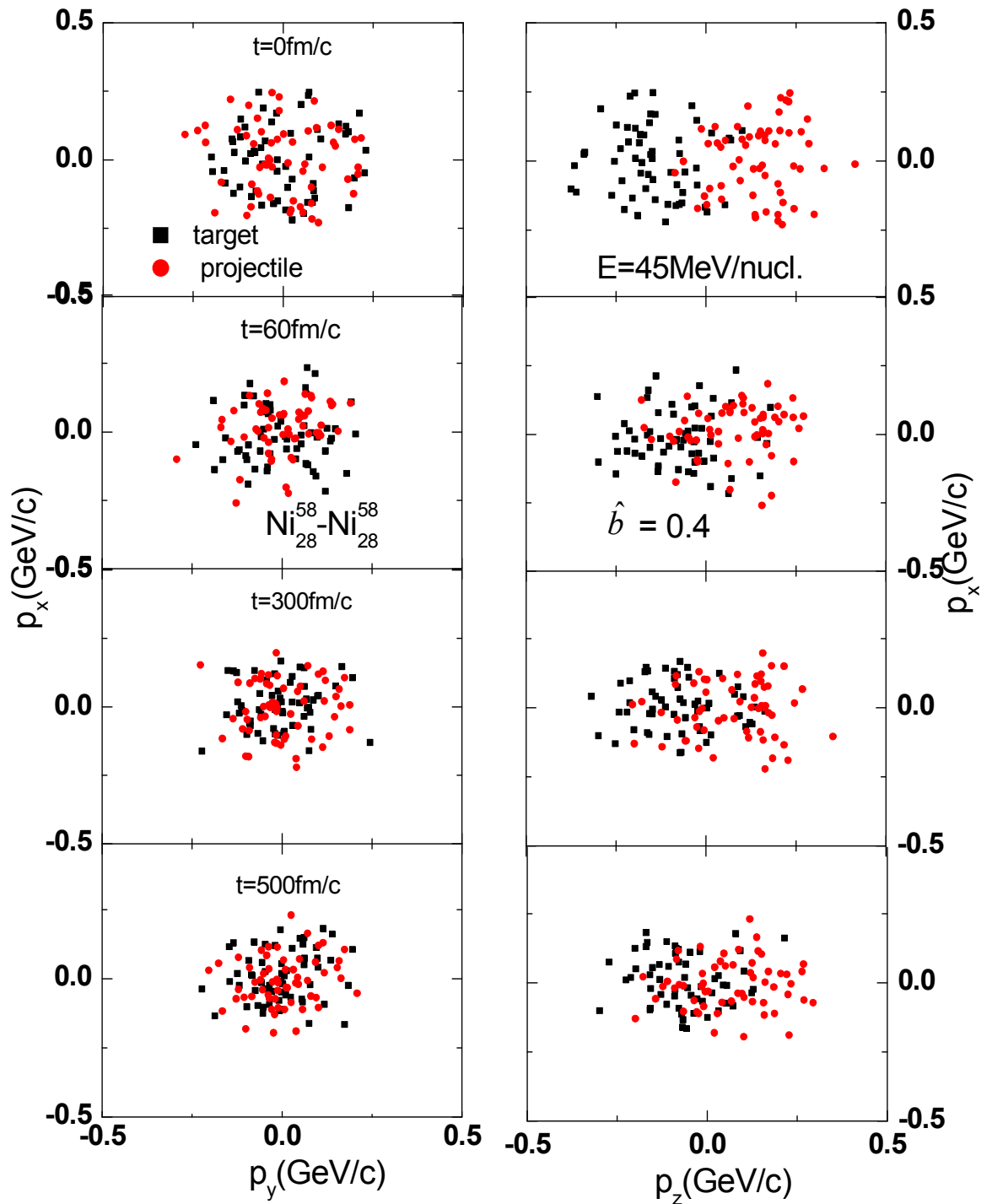


Figure 3.2: Same as fig. 3.1 but in momentum space.

After the collision, the formation of light particles and heavy fragments can be seen. In contrast, the momentum space is less affected. The beam energy is too small to allow nucleon-nucleon collision to take place and hence no substantial change in momentum space occurs.

The next stage in the reaction scenario is the relaxation of the energy density. The central system (at time 60fm/c) is undergoing expansion, thereby reducing its temperature and density. Due to frequent nucleon-nucleon collisions, nucleons scatter in the radial direction. With the evolution of the reaction, participant matter increases, leading to more nucleons scattering in the radial direction. Therefore, after the collision, the formation of light particles and heavy fragments can be seen [1-3]. At the end of the reaction, we see only few spectator nucleons. Looking at the momentum space (Fig. 3.2), we see that the spectator nucleons have very little change in their initial velocity profile over the period of reaction.

On the other hand, participant matter pushes the nucleon into midrapidity region, therefore, driving the system into global equilibrium. Naturally, more initial correlations are destroyed, more is the system close to global equilibrium. Since, these figures are the snapshots of a single event, the picture could be slightly different for different events. In the final state, matter is cold and fragmented, therefore, this may lead to the expansion of compressed matter which breaks into pieces due to Coulomb instabilities. The system always expands into the direction of the largest gradients in density and temperature.

The reaction stops at a point commonly referred to as freeze-out. At this point the densities are small enough that during a typical path length no further interaction will occur. Our phase space is similar to phase space shown in ref. [4, 5, 6].

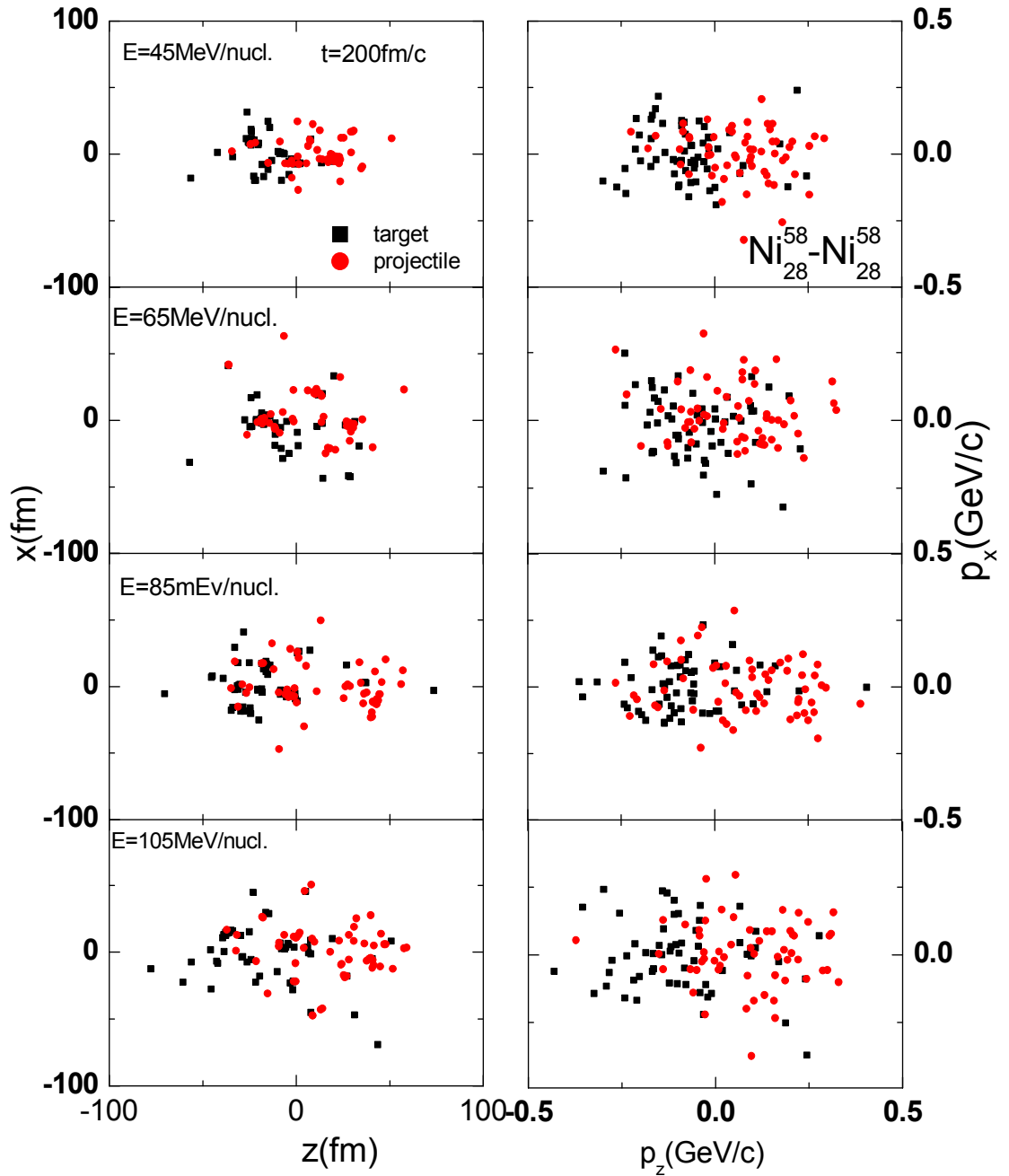


Figure 3.3: The projection of the phase-space in  ${}_{28}\text{Ni}^{58}+{}_{28}\text{Ni}^{58}$  collisions in special and momentum space in  $(x-z)$  and  $(P_x-P_z)$  planes.

The role of different incident energies is displayed in figure 3.3 where the X-Z &  $P_x - P_z$  coordinates of all nucleons are plotted at 200 fm/c. A very heavy fragment can be seen at 45 MeV/nucl. This disappears at higher incident energies. At 105MeV/nucleon, nearly no Heavy fragment survives. In other words, the present figure depicts that at low incident energies, a partial fusion can occur whereas at higher energies either emission of the light fragments or free nucleons will dominate the reaction. Such change in fragment sizes also occurs with change in incident energies of projectile [7].

### **3.3 Time Evolution**

In heavy-ion collisions, figure 3.4 sketches schematically a typical heavy-ion reaction. When two nuclei approach each other, their orientation in space and the initial beam direction define the reaction plane. The impact parameter vector beam is located in the reaction plane.

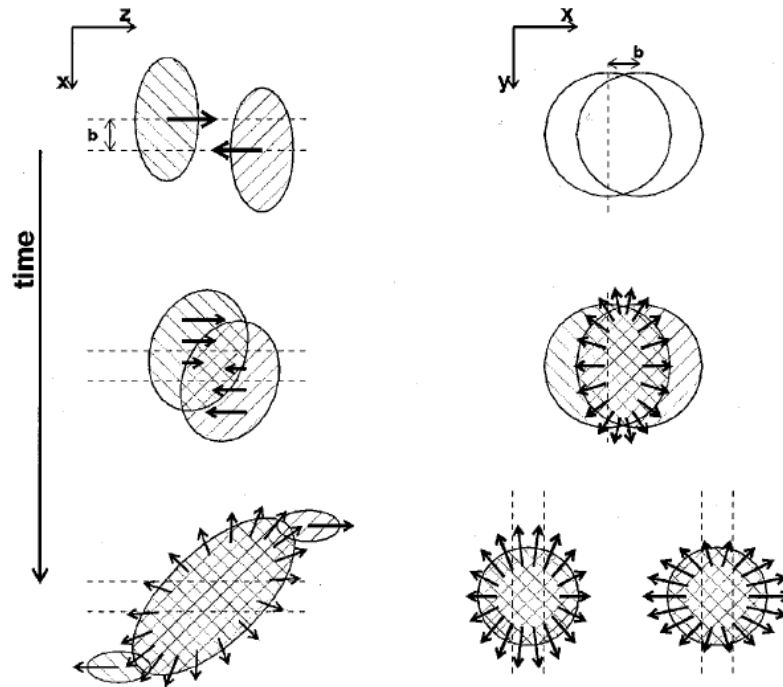


Figure 3.4: Schematic view of the time evolution in a heavy-ion collision.

**(1) Initial Phase:** When the two matter distributions approach each other and start to overlap, the properties of the NN interaction in free space will be visible in the scattering process. Nucleons at the surfaces will reflect the Lorentz-force-like behavior of the NN interaction most directly. They will be deflected outward and, because of symmetry for finite impact parameter, will show an enhancement in the reaction plane.

**(2) High Density Phase:** Once the matter distributions of the projectile and target overlap (Figure 3.4, central row), the properties of the NN interaction are not well known. At incident beam energies that exceed the velocity of sound in nuclear matter at ground-state nuclear-matter density ( $\rho_s = 2$ ), the nucleons cannot escape fast enough and a zone of high density is formed. Many-body effects that are present even at normal nuclear-matter densities can occur, as well as modifications of the properties of the constituents (medium effects).

**(3) Expansion:** The next stage in the reaction scenario is the relaxation of the energy density. The central system is undergoing expansion, thereby reducing its temperature and density. For symmetric collisions, the expansion is azimuthally symmetric for central collisions. For reactions with finite impact parameter, where an oriented velocity field might have survived the compression phase, the situation is much more complicated. The expansion now has a directed velocity field superimposed (Figure 3.1, lower left). The system always expands into the direction of the largest gradients in density and temperature. Inspection of the geometry depicted in Figure 3.1 reveals that, in transverse direction, the initial expansion is largest in the direction of the reaction plane. In longitudinal direction, the expansion scenario depends on the degree of stopping. For a high degree of stopping and given the fact that the nuclei are Lorentz contracted in this direction, the pressure gradient is largest along the beam direction; therefore, the system relaxes predominantly longitudinally.

**(4) Freeze-Out:** The reaction stops at a point commonly referred to as freeze-out. At this point the densities are small enough that during a typical path length no further interaction will occur.

One of the motivations behind studying a heavy-ion collision is to extract the information regarding the hot and dense nuclear matter. In our approach, the matter density is calculated as [8]

$$\rho(\vec{r}, t) = \sum_{i=1}^{A_T+A_P} \frac{1}{(2\pi L)^{3/2}} e^{-(r-r_i(t))^2/2L} \quad (3.1)$$

Here  $A_T$  and  $A_P$  stand, respectively, for the target and projectile. In actual calculations, we take a sphere of 4 fm radius around the center-of-mass and compute the density at each time step during the reaction using eq. (3.1).

The important quantity directly linked with the density is the collision rate. In fig. 3.4 we display the time evolution of  $dN_{coll}/dt(\text{allowed})$ . This rate represents the net collisions after fulfilling the Pauli principle. Naturally, the attempted rate will be much higher than the allowed one.

Fig. 3.5 Shows the rate of collisions at different bombarding energies. We notice that rate of collision is intimately related to violence of collision. Here initially there is no collision among the nucleon [9, 10]. At time 30fm/c compound nuclear matter will form. There is maximum compression among the nucleons at this time. With the evolution of time the matter expands and breaks into fragments (consisting of the entities of all sizes). The preservation of the initial nucleon-nucleon correlations can be linked with the collision rate which is displayed in this figure. The maximal collision rate, which lasts longer in heavier colliding nuclei, will not allow the fragment distribution to saturate for long time. In other words, the saturation time of the fragmentation yield will be shorter in lighter systems. Here the saturation time is nearly 200fm/c in all energy ranges. After this time there will be no further collision. We notice that the rate of collisions increases with increase in energy.

It is observed that the rate of collision is increasing with increase in the incident energy. This is due to increase in compression with incident energy.

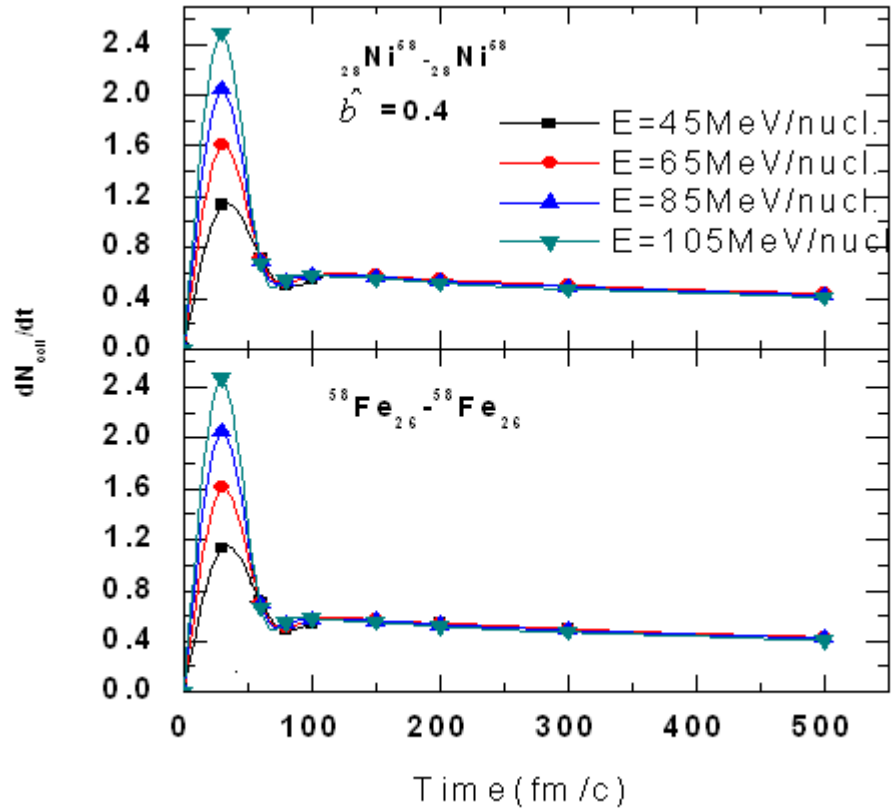


Fig 3.5. The rate of allowed nucleon-nucleon collisions as a function of time for

$${}_{28}\text{Ni}^{58}+{}_{28}\text{Ni}^{58} \quad \text{and} \quad {}_{26}\text{Fe}^{58}+{}_{26}\text{Fe}^{58}.$$

Interestingly, the rate of collision is more for neutron poor (proton-rich) system  ${}_{28}\text{Ni}^{58}+{}_{28}\text{Ni}^{58}$  is due to effect of more coulomb repulsion in the presence of large number of protons, which are 28 in case of Ni and 26 in case of Fe.

In summary, one is able to observe the effect of low as well as intermediate energies in the phase-space in (X-Z) as well as (  $P_X$ - $P_Z$  ) planes. This is indirectly the fusion-fission processes at low incident energies, while propagation at higher energies. Moreover the  $N/P$  ratio is found to be sensitive towards the rate of allowed collisions indicating the existence of isospin effects at intermediate energies.

### **3.4 References:**

[1] S.Kumar & R.K. Puri, Physical Review C, Volume **60**, 054607 (1999).

- [2] J. Singh, S. Kumar & R.K. Puri, Phys. Rev. C. Volume **63**, 054603 (2001).
- [3] S. Kumar & R.K. Puri, Phys. Rev. C **58**, 320 (1998).
- [4] R. K. Puri & J. K. Dhawan, Eur. Phys. J. A. **33**, 57-64 (2007).
- [5] R. K. Puri & J. K. Dhawan, Physical Review **74**, 054610 (2006).
- [6] R. K. Puri & J. K. Dhawan, Physical Review **75**, 057601 (2007)
- [7] P.B. Gossia, R.K. Puri, C.Hartnak & J. Aichelin, Nucl. Phys. A **619**, 379 (1997).
- [8] D.T. Khoa et al. Nucl. Phys. A 548, 102 (1992); R.K. Puri et al., Nucl. Phys. A 575, **733** (1994).
- [9] A.D. Sood and R.K. Puri, Phys. Rev. C **70**, 034611 (2004).
- [10] B. Blattel et. Al. Phys. Rev. C **43**, 2728 (1991).

## CHAPTER 4

### DIRECTED FLOW

#### 4.1 Introduction

The collective transverse in-plane flow [1–3] has been used extensively over the past three decades to study the properties of hot and dense nuclear matter, i.e. the nuclear matter equation of state (EOS) as well as the in-medium nucleon-nucleon (nn) cross section. The dependence of the collective flow on the above-mentioned parameters has revealed much interesting physics, especially the beam energy dependence which has also lead to its disappearance. At lower incident energies, the dominance of the attractive mean field prompts the scattering of the particles into negative deflection angles thus producing negative flow whereas frequent NN collisions at higher incident energies result in the emission of particles into positive deflection angles and hence yield positive flow. While going through the incident energies, collective transverse in-plane flow disappears at a particular incident energy termed as the balance energy ( $E_{bal}$ ) or energy of vanishing flow (EVF).

#### 4.2 Directed flow

The transverse flow is a collective sidewise-deflection of forward and backward moving particles within the reaction plane. The sideward flow is often represented in terms of the average in-plane transverse momentum at a given rapidity [4].

$$y(i) = \frac{1}{2} \ln \frac{E(i) + P_x(i)}{E(i) - P_x(i)}$$

Where  $E(i)$  is the energy of  $i^{\text{th}}$  particle and  $P_x(i)$  is the transverse momentum of particle in the reaction plane. The transverse flow has been a major tool for investigating the EOS of hot and dense matter as well as in medium nucleon-nucleon cross section. It was first pointed out that the transverse flow depends on the isospin asymmetry of the

reaction system. Furthermore, the so-called balance energy ( $E_{bal}$ ), where the attractive part of the nuclear interactions balances the repulsive part.

Presently, due to availability of radioactive beams, role of isospin degree of freedom in EOS can be studied. The collective transverse in-plane flow (directed flow) has been found to depend on isospin of colliding system. Here we aim to study the dependence of balance energy on isospin using IQMD model.

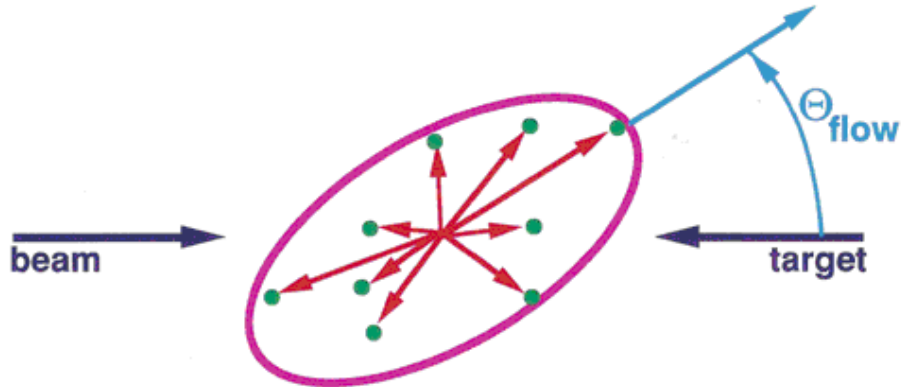


Fig.4.1 Directed flow

### **4.3 Why there is difference in balance energies of symmetric system?**

Before we proceed to show our numerical results, it is appropriate to attempt to understand the reasons why we would expect a difference in the balance energy for symmetric systems of equal mass, with different neutron and proton numbers. There are three isospin effects that we may consider [5]:

- 1) The average effective nucleon-nucleon cross section,
- 2) Difference in the Coulomb potential, and
- 3) The isospin dependence of the mean field.

In order to understand the sign of the different effects, we first remind ourselves that the balance energy marks the beam energy at which the repulsive and attractive interactions are roughly equal. At beam energies lower than the balance energy, the attractive interaction dominates, and at energies higher than the balance energy, repulsive interactions determine the flow.

### **(1)Effect of coulomb potential**

The difference in the Coulomb interaction is very simple. Fe has 26 protons and Ni 28. This means that the ratio of the Coulomb forces is  $(26/28)^2 = 0.862$ . Since the Coulomb force adds repulsion, we thus expect that the balance energy for nickel should be lower than that for iron.

### **(2)Effect mean field potential**

The difference in the isospin dependent mean field has the opposite effect. The isospin asymmetry,  $\delta$ , is three times bigger for iron than it is for nickel.

$$\delta ({}_{26}\text{Fe}^{58}) = 0.103, \delta ({}_{28}\text{Ni}^{58}) = 0.034$$

A larger isospin asymmetry results in more repulsion.

### **(3)Effect of average effective nucleon-nucleon cross section**

The numbers of protons and neutrons in the colliding system also have an influence on the average nucleon-nucleon cross section, because the neutron-proton cross section is approximately a factor of 3 times bigger than the proton-proton cross section in the energy regime of interest here. We can then calculate the average nucleon-nucleon cross section from the number of collisions between nucleons of equal and opposite isospin,

$$\begin{aligned}\sigma &= \frac{N_{np} \sigma_{np} + (N_{nn} + N_{pp}) \sigma_{pp}}{N_{np} + N_{nn} + N_{pp}} \\ &= \frac{3N_{np} + N_{nn} + N_{pp}}{N_{np} + N_{nn} + N_{pp}} \sigma_{pp}\end{aligned}$$

Where  $N_{np}$  is the number of neutron-proton collisions. Thus  $E_{bal}$  for  ${}_{26}\text{Fe}^{58} + {}_{26}\text{Fe}^{58}$  has been found to be higher than  ${}_{28}\text{Ni}^{58} + {}_{28}\text{Ni}^{58}$ . This is because of difference in cross-sections for different nucleons. The neutron-proton cross-section is approximately three times higher than proton-proton and neutron-neutron cross –section. This leads to less repulsive flow in more neutron rich system, hence fourth increasing the balance energy in neutron rich system.

## 4.4 Results and disscussion

We have simulated the reactions of at incident energies ranging from 45MeV/neuclon to 175 MeV/neucleon in small steps .The reactions are simulated at scaled impact parameter of  $\hat{b} = 0.2, 0.4, 0.5, 0.6,$  and  $0.7$  using soft EOS without momentum dependence.

The reactions are followed till the transverse flow saturates. The saturation time is around 200 fm/c for the reactions in the present study. There are several methods in literature to define the nuclear transverse in-plan flow. In most of studies, the EVF is extracted from  $(P_x/A)$  plots where one plots  $(P_x/A)$  as a function of  $Y_{c.m}/Y_{beam}$ . Using the linear fit to the slope, one can find the so called reduced flow. Naturally the energy at which the reduced flow passes through zero is called EVF. Alternatively, one can also use a more integrated quantity ‘‘directed transverse momentum  $\langle P_x^{dir} \rangle$  ‘‘ which is defined as [5-11, 14]

$$\langle P_x^{dir} \rangle = \frac{1}{A} \sum_{i=1}^A \text{sign}\{y(i)\} P_x(i) ,$$

Where  $y(i)$  and  $P_x(i)$  are respectively, the rapidity and momentum of  $i^{th}$  particle.

In fig.4.2.&4.3, average  $\langle p_x/A \rangle$  (MeV/c) as a function of scaled rapidity  $y_{c.m}/y_{beam}$  is shown. We display the results at impact parameters  $\hat{b} = 0.2, 0.4, 0.5, 0.6$  and  $0.7$ (taken from ref.8). In all the cases, + ve to – ve transition is observed for all impact–parameters upto 85Mev/nucleon. However at higher energies, -ve to +ve transition is observed for  $\hat{b} =0.2$  (central collisions). This is indicated that the balance energy for  $\hat{b} =0.2$  is between 85 to 95Mev/nucleon. Moreover with increase in impact-parameter, the slope is increasing at all incident energies. From here it is clear that balance energy is sensitive towards the impact-parameter or geometry of reaction [12, 15].

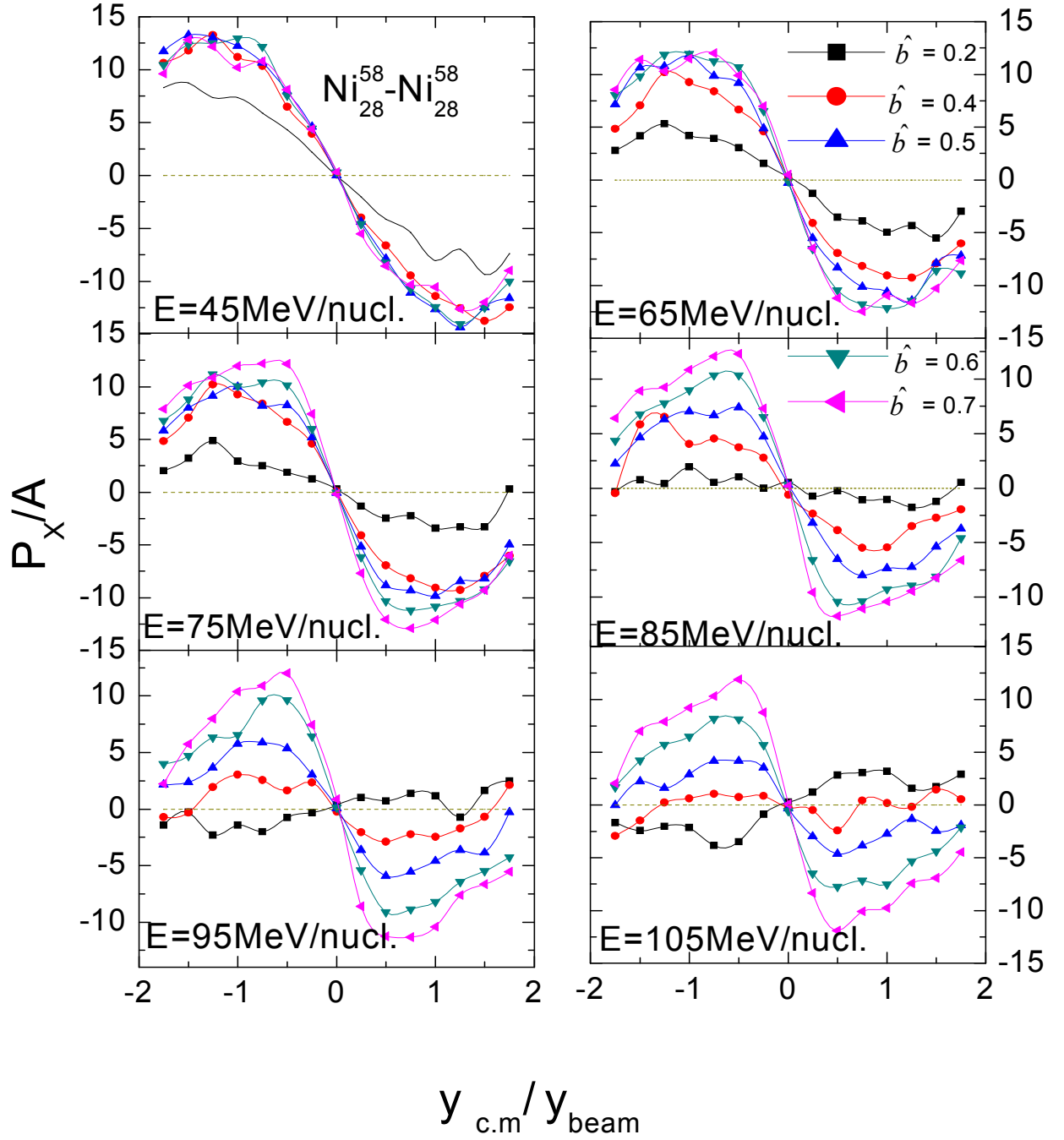


Fig 4.2 The averaged  $P_x/A$  as a function of  $Y_{c.m.}/Y_{beam}$  with  $\sigma=80\%$  of free cross section.

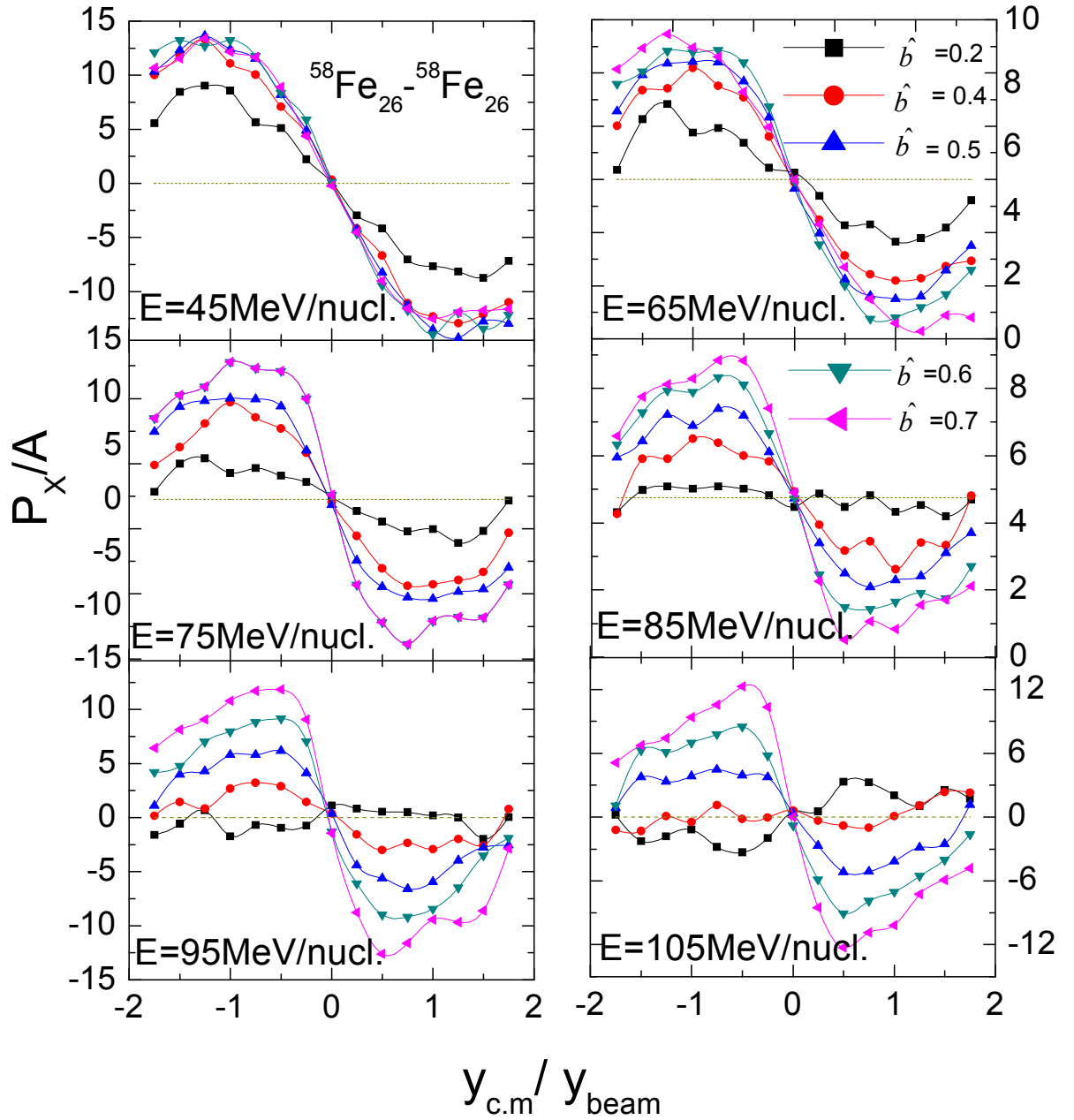


Fig.4.3 same as fig 4.2 but for  ${}_{26}\text{Fe}^{58}+{}_{26}\text{Fe}^{58}$  system.

Fig. 4.4. & 4.5 the time evolution of directed flow  $\langle P_x^{\text{dir}} \rangle$  is displayed at different impact-parameters ranging from  $(\hat{b} = 0.2$  to  $0.7)$ . The panels in the figure are at different incident energies ranging from  $45 \text{ MeV/nucl.}$  to  $105 \text{ MeV/nucl.}$

The  $\langle P_x^{\text{dir}} \rangle$  is changing from – ve to + ve value only for  $\hat{b} = 0.2$  ( central collisions) between 85 to 95MeV/nucleon. The  $\langle P_x^{\text{dir}} \rangle$  is becoming more negative with increase in impact parameter indicating the dominance of attractive mean field. Moreover with increase in incident energy becoming less negative indicating the dominance of nucleon-nucleon collision. This is true for fig 4.4 and 4.5. It is observed that  $\langle P_x^{\text{dir}} \rangle$  is more negative for more neutron – rich systems compared to neutron-poor system indicating the higher value of balance energy for neutron-rich system. In order to confirm these findings in fig 4.5 & 4.6 incident energy as well as impact parameter dependence of directed flow is displayed.

If one compares the fig 4.2 and 4.3 and 4.4 with 4.5, the shape of lines are similar in both the figures. The difference observed is in the magnitude of  $P_x/A$ . The  $P_x/A$  is becoming more positive for neutron – rich system  ${}_{26}\text{Fe}^{58}$  as compared to neutron-poor system  ${}_{28}\text{Ni}^{58}$ . This is indicating towards the higher value of balance energy for  ${}_{26}\text{Fe}^{58}$  system. This study can be further established with the other parameter.

In Fig.4.6 In order to evaluate balance energy in fig 4.4 & 4.5, the excitation function of directed flow is displayed at different impact-parameters for  ${}_{28}\text{Ni}^{58}+{}_{28}\text{Ni}^{58}$  and  ${}_{26}\text{Fe}^{58}+{}_{26}\text{Fe}^{58}$  systems. The directed flow is increasing with increase in incident energy. A point comes at which directed flow crosses from –ve to +ve value. This point is found to vary with impact-parameter. With increase in impact-parameter the system is enjoying more in mean field as compared to NN collision. It is clear that balance energy is increasing with increase in impact-parameter. The main interest is to prove the shift in balance energy due to increase in number of neutrons. The experimental data is also available for balance energy (at which  $\langle P_x^{\text{dir}} \rangle \rightarrow 0$ ) [9].

In fig.4.6. At different impact-parameters, balance energy is taken and then plotted the impact parameters dependence of balance energy in fig 4.7. Here the mean field occurs below balance energy and collisions occur above balance energy. In order to determine the balance energy, the energy is varied between these two values and a linear fit is applied to the slopes of distributions. The balance energy is different for different impact parameters. The value of balance energy ( $E_{\text{bal}}$ ) increases with increase in impact-parameter. In case of  ${}_{28}\text{Ni}^{58}+{}_{28}\text{Ni}^{58}$  having lesser no of neutrons (having lesser repulsion) has balance energy lesser as compared to  ${}_{26}\text{Fe}^{58}+{}_{26}\text{Fe}^{58}$ .

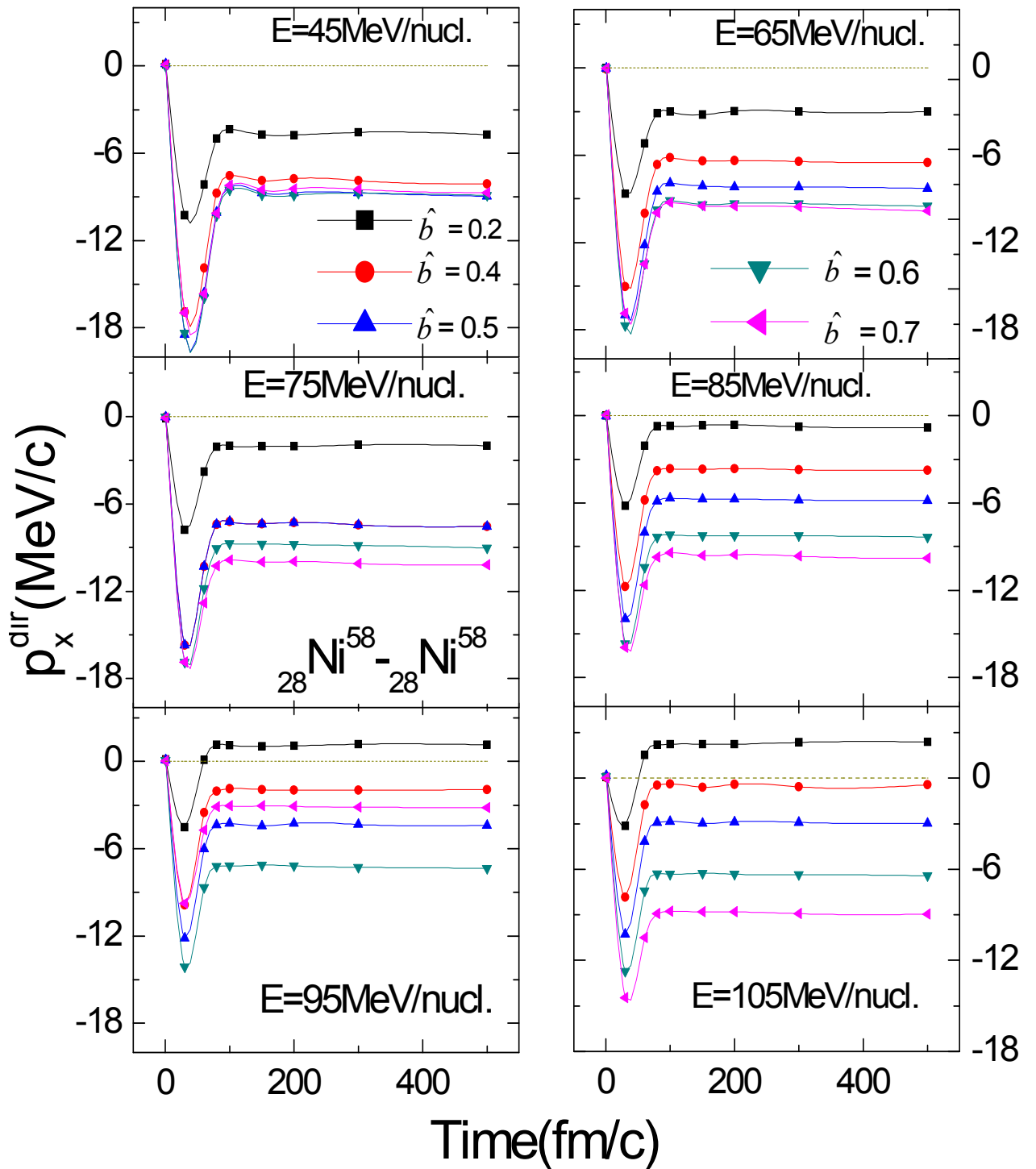


Fig. 4.4 The Time evolution of  $\langle P_x^{\text{dir}} \rangle$  instead of  $P_x/A$  is plotted quite similar trends.

Here  $\langle P_x^{\text{dir}} \rangle$  is placed as a function of reaction time.

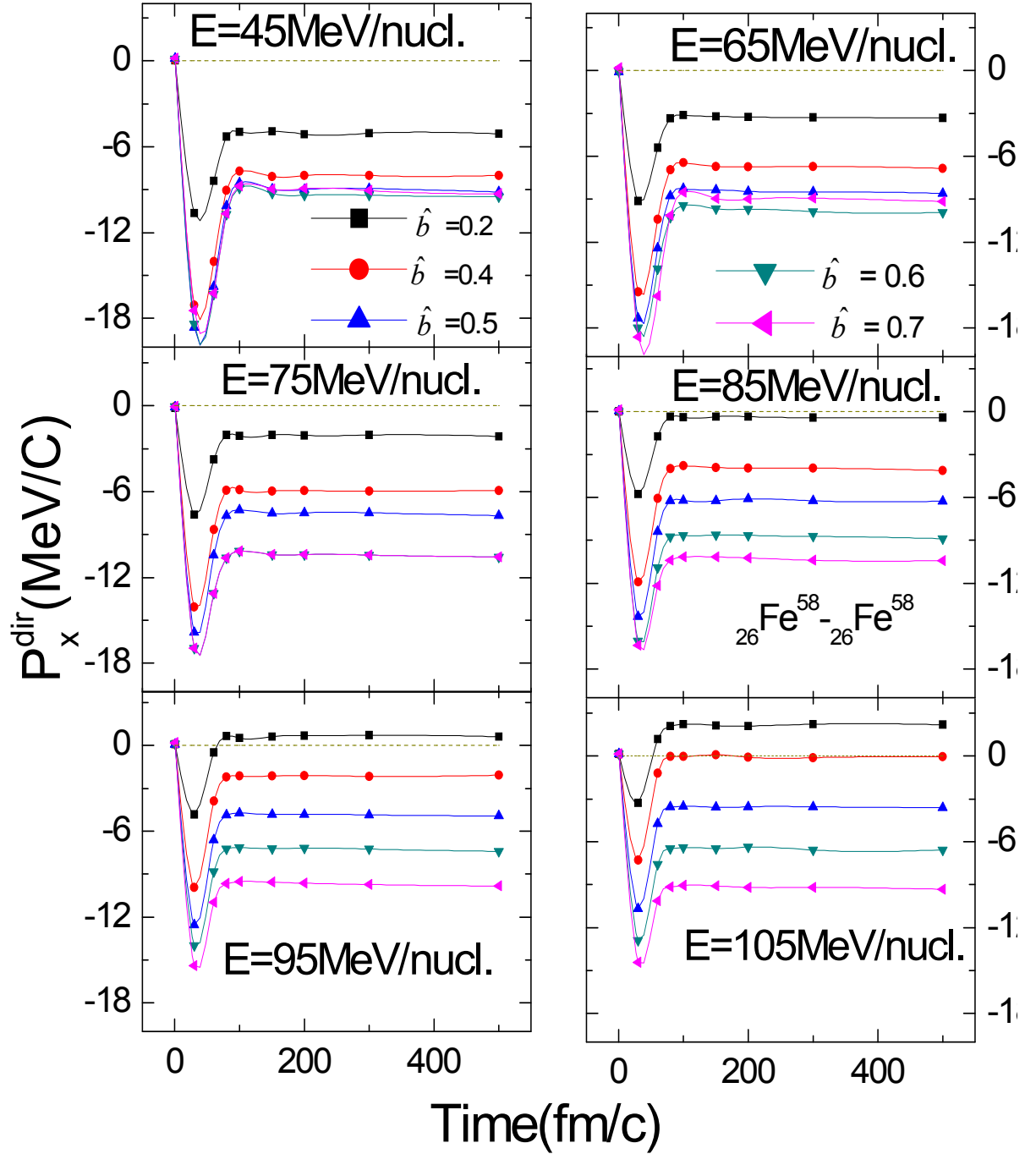


FIG.4.5. same as fig. 4.4 but for  ${}_{26}\text{Fe}^{58}+{}_{26}\text{Fe}^{58}$  system.

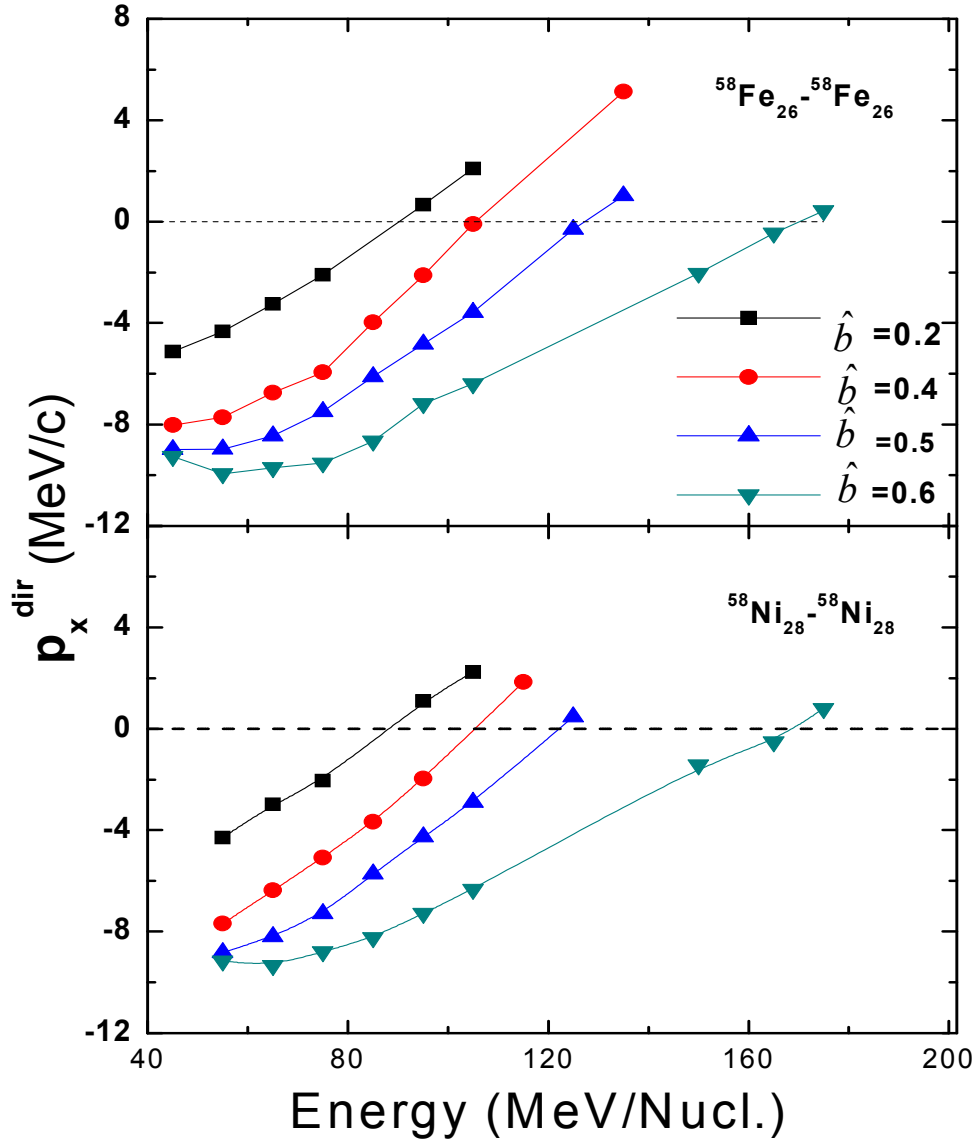


FIG.4.6 shows  $\langle p_x^{dir} \rangle$  as a function of incident energy for  ${}_{26}\text{Fe}^{58}+{}_{26}\text{Fe}^{58}$  and  ${}_{28}\text{Ni}^{58}+{}_{28}\text{Ni}^{58}$ .

Fig 4.7. Depicts the impact parameter dependence of balance energy for the system of  ${}_{28}\text{Ni}^{58}+{}_{28}\text{Ni}^{58}$  and  ${}_{26}\text{Fe}^{58}+{}_{26}\text{Fe}^{58}$ . An increase of balance energy with impact parameter is visible. At large impact parameter fewer nucleon-nucleon collisions yield reduced repulsive forces. Therefore the attractive mean field dominates. The trends in the values of  $E_{bal}$  with isospin dependence are consistent with those for the measured values predicted by BUU model as well as with IQMD model. The balance energy increases as a

function of impact parameter for both isotropic systems, and  $E_{\text{bal}}$  (symmetry energy) is systematically higher for more neutrons rich system at all impact parameter bins, as compared to neutron-poor system. This is due to isospin effects and due to cross-section effects which are discussed earlier in this chapter. Same types of findings are also observed by experimentalists. We are very close to the trend, but not close to experimental values. By reducing the cross-section value  $\sigma = 0.8\sigma_{\text{free}}$  which is also reduced in likewise a few times [11, 12-14].

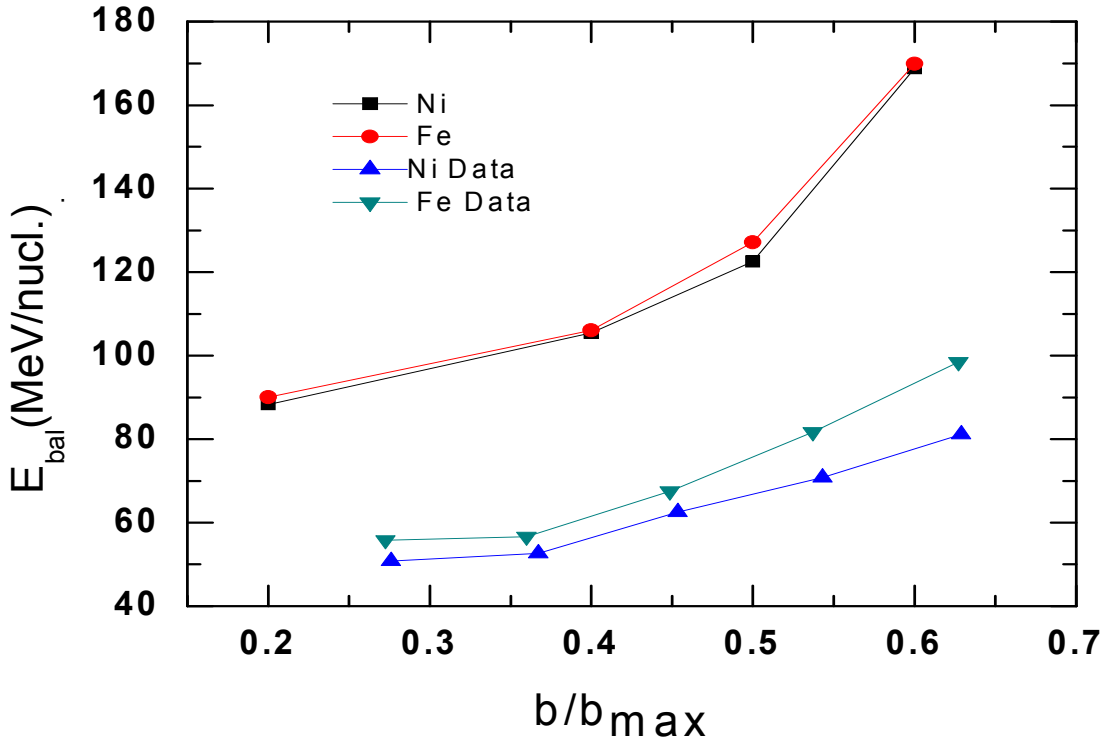


FIG.4.7 Measured balance energies as a function of impact parameter for  ${}_{26}\text{Fe}^{58}+{}_{26}\text{Fe}^{58}$  ( ${}_{28}\text{Ni}^{58}+{}_{28}\text{Ni}^{58}$ ).

## 4.5 References :

- [1] Scheid W, Muller H and Greiner W 1974 Phys. Rev. Lett. **32** 741(1997)
- [2] Gustafsson H. A et. al. 1984 Phys. Rev. Lett. **52** 1590

- [3] Doss K G R et al 1986 Phys. Rev. Lett. **57** 302
- [4] Aman D. Sood and Rajeev K. Puri Phys. Rev C **70**, 034611(2004).
- [5] E. Lehmann, A. Faessler, J. Zipprich, R. K. Puri, and S. W.Huang, Z. Phys. A **355**, 55 (1996).
- [6] S. Kumar, M. K. Sharma, R. K. Puri, K. P. Singh, and I. M.Govil, Phys. Rev. C **58**, 3494 (1998).
- [7] A. Sood and R. K. Puri, Symposium on Nuclear Physics, 2002, Vol. 45B, P. 288; A. Sood and R. K. Puri, Proceedings of the VIII International Conference on Nucleus-Nucleus Collisions, Moscow, Russia, 2003 (unpublished).
- [8] Sakshi Gautam, Rajeev Chugh, Aman D.Sood,Rajeev K.Puri,Ch.Hartnack,J.Aichelin Nucl.Part. Physics **37**,085102 (2010).
- [9] S. Kumar, R. K. Puri, and J. Aichelin, Phys. Rev. C **58**, 1618(1998).
- [10] J. Aichelin, Phys. Rep. **202**, 233 (1991); J. Aichelin and H.Stöcker, Phys. Lett. B **176**, 14 (1986).
- [11] C. Hartnack, R. K. Puri, J. Aichelin, J. Konopka, S. A. Bass,H. Stöcker, and W. Greiner,Eur. Phys. J. A **1**, 151 (1998).
- [12] B. Blättel, V. Koch, A. Lang, K. Weber, W. Cassing, and U.Mosel, Phys. Rev. C **43**, 2728 (1991).
- [13] G. D. Westfall et al., Phys. Rev. Lett. **71**, 1986 (1993).
- [14] Sakshi Gautam, Rajiv Chugh, Aman D. Sood, Rajeev K. Puri, Ch.Hartnack and J.Aichelin 1443, **2**(2010).
- [15] D. J. Magestro, W. Bauer, O. Bjarki, J. D. Crispin, M. L. Miller, M. B. Tonjes, A. M.Vander Molen, and G. D. Westfall Phys. Rev. C, **61**, 021602R (2000).

## CHAPTER 5

### SUMMARY

---

This thesis contains a theoretical study of transverse flow in heavy ion nuclear reactions. The IQMD model is used to study the transverse flow for projectile and target  ${}_{28}\text{Ni}^{58}+{}_{28}\text{Ni}^{58}$  and  ${}_{26}\text{Fe}^{58}+{}_{26}\text{Fe}^{58}$  at  $E = 45, 65, 85, 105$  MeV/nucleon and scaled impact parameter  $\hat{b} = 0.2, 0.4, 0.5, 0.6, 0.7$ . The details of different theoretical models were discussed in Chap. 2. We discussed in particular, isospin quantum molecular dynamics model and IBUU model.

In chapter 3, the time evolution of  ${}_{28}\text{Ni}^{58}+{}_{28}\text{Ni}^{58}$  collisions in coordinate and momentum space respectively. Through this study, we analysed the processes involved in non-central heavy ion collisions which include the formation of initial phase, high density phase, expansion and freeze-out. The evolution of the rate of nucleon-nucleon collisions as a function of time was also done.

In chapter 4, we have attempted to understand the nature of transverse flow in  ${}_{28}\text{Ni}^{58}+{}_{28}\text{Ni}^{58}$  and  ${}_{26}\text{Fe}^{58}+{}_{26}\text{Fe}^{58}$  systems at wide range of energies and impact parameters. The isospin dependence of balance energy in transverse flow is clearly visible. The results are compared with experimental data available.